https://doi.org/10.5194/hess-2019-337
Preprint. Discussion started: 29 July 2019

Hydrology and Earth System Sciences
Discussions

Freshwater pearl mussels from northern Sweden serve as long-term, high-resolution stream water isotope recorders

Bernd R. Schöne[1], Aliona E. Meret[2], Sven M. Baier[3], Jens Fiebig[4], Jan Esper[1], Jeffrey McDonnell[5], Laurent Pfister[6]

[1]Institute of Geosciences, University of Mainz, Mainz, 55128, Germany
[2]Naturhistoriska riksmuseet, Stockholm, 114 18, Sweden
[3]Agilent Technologies Sales & Services GmbH & Co.KG, Frankfurt/M., 60528, Germany
[4]Institute of Geosciences, J.W. Goethe University, Frankfurt/M., 60438, Germany
[5]Global Institute for Water Security, University of Saskatchewan, Saskatoon, SK S7N 3H5, Canada
[6]Department 'Environmental Research and Innovation', Luxembourg Institute of Science and Technology, Belvaux, 4422, Grand-Duchy of Luxembourg

Correspondence to: Bernd R. Schöne (schoeneb@uni-mainz.de)

Abstract. The stable isotope composition of lacustrine sediments is routinely used to infer Late Holocene changes in precipitation over Scandinavia and ultimately, atmospheric circulation dynamics in the North Atlantic realm. However, such archives provide only low temporal resolution (ca. 15 years) precluding the ability to identify changes on inter-annual and quasi-decadal time-scales. Here we present a new, high-resolution reconstruction using shells of freshwater pearl mussels, *Margaritifera margaritifera*, from three rivers in north Sweden. We present seasonally to annually resolved, calendar-aligned stable oxygen and carbon isotope data from ten specimens covering the time interval of 1819 to 1998. The studied bivalves formed their shells near equilibrium with the oxygen isotope signature of ambient water and thus reflected hydrological processes in the catchment as well as changes, albeit damped, of the isotope value of local atmospheric precipitation. Shell oxygen isotopes were correlated significantly with the North Atlantic Oscillation index (up to 56 % explained variability) suggesting that moisture from which winter precipitation formed originated predominantly in the North Atlantic during NAO^+ years, but in the Arctic during NAO^- years. The specific isotope signature of winter precipitation was damped in stream water and this effect was recorded by the shells. Shell stable carbon isotope values did not show consistent ontogenetic trends, but rather oscillated around an average that differed slightly among the studied rivers (ca. -12.00 to -13.00 ‰). Results of this study contribute to an improved understanding of climate dynamics in Scandinavia and the North Atlantic sector and can help to constrain ecological changes in riverine ecosystems. Moreover, long isotope records of precipitation and streamflow are pivotal for improving our understanding and modeling of hydrological, ecological, biogeochemical and atmospheric processes. Our new approach offers a much higher temporal resolution and superior dating control than existing archives.

https://doi.org/10.5194/hess-2019-337
Preprint. Discussion started: 29 July 2019

Hydrology and Earth System Sciences
Discussions

1 Introduction

Multi-decadal records of $\delta^{18}O$ signals in precipitation and stream water are important for documenting climate change impacts on river systems (Rank et al., 2017), improving mechanistic understanding of water flow and quality controlling processes (Darling and Bowes, 2016) and testing earth hydrological and land surface models (Reckerth et al., 2017; Risi et al., 2016). However, the common sedimentary archives used for such purposes typically do not provide the required temporal resolution (e.g., Rosqvist et al., 2007). In such studies, the temporal changes in the oxygen isotope signatures of meteoric water are encoded in biogenic tissues and abiogenic minerals formed in rivers and lakes (e.g., Teranes et al. 2001; Leng & Marshall 2004). In fact, many studies have determined the oxygen isotope composition of diatoms, ostracods, authigenic carbonate and aquatic cellulose preserved in lacustrine sediments to reconstruct Late Holocene changes in precipitation over Scandinavia and ultimately, atmospheric circulation dynamics in the North Atlantic realm (e.g., Hammarlund et al., 2002; Andersson et al., 2010; Rosqvist et al., 2004, 2013). With their short residence times (Rosqvist et al., 2013), the small, hydrologically connected, through-flow lakes of northern Scandinavia are an ideal region for this type of study. Their isotope signatures – though damped in comparison to isotope signals in precipitation – directly respond to changes in precipitation isotope composition (Leng & Marshall 2004). However, even the highest available temporal resolution of such records (15 years per sample in sediments from Lake Tibetanus, Swedish Lappland; Rosqvist et al., 2007) is still insufficient to resolve inter-annual to decadal-scale variability, i.e., the time-scales at which the North Atlantic Oscillation (NAO) operates (Hurrell, 1995; Trouet et al., 2009). The NAO steers weather and climate dynamics in northern Scandinavia and determines the origin of air masses from which meteoric waters form. While sediment records are still of vital importance for century and millennial-scale variations, new approaches are needed for finer scale resolution on the 1–100-year time-scale.

One new approach for hydroclimate reconstruction is the use of freshwater mussels as natural stream water stable isotope recorders (Dettman et al., 1999; Kelemen et al., 2017; Pfister et al., 2018, 2019). Their shells can provide seasonally to annually resolved, chronologically precisely constrained records of environmental changes in the form of variable increment widths (= distance between subsequent growth lines) and geochemical properties (Nyström et al. 1996; Schöne et al. 2005a; Schöne and Krause, 2016; Geeza et al., in press a, b; Kelemen et al., in press). In particular, as almost all other bivalves, freshwater mussels form their shells near equilibrium with the oxygen isotope signature of the water in which they live (Dettman et al., 1999; Kaandorp et al. 2003; Versteegh et al. 2009; Kelemen et al., 2017). Freshwater pearl mussels, *Margaritifera margaritifera*, are particularly useful in this respect, because they can reach a lifespan of over 200 years (Ziuganov et al. 2000; Mutvei & Westermark 2001) offering an insight into long-term changes of freshwater ecosystems at unprecedented temporal resolution.

Here we present the first, absolutely dated, annually resolved stable oxygen and carbon isotope record of freshwater pearl mussels from three different rivers in northern Sweden covering nearly two centuries (1819–1998). We test the ability

https://doi.org/10.5194/hess-2019-337
Preprint. Discussion started: 29 July 2019

Hydrology and Earth System Sciences
Discussions

of these freshwater pearl mussels to reconstruct the NAO index and associated changes in precipitation provenance using shell oxygen isotope data ($\delta^{18}O_s$). We evaluate how shell oxygen isotope data compares to $\delta^{18}O$ of stream water ($\delta^{18}O_w$) and precipitation ($\delta^{18}O_p$) and how the latter two relate to each other. In addition, we explore the physical controls on shell stable carbon isotope signatures. We leverage past work in Sweden that has shown that the main growing season of *M. margaritifera* lasts from mid-May to mid-October, with fastest growth rates occurring between June and August (Dunca & Mutvei, 2001; Dunca et al. 2005; Schöne et al., 2004a, b, 2005a). We use changes in annual increment width of *M. margaritifera* to infer water temperature, because growth rates are faster during warm summers and result in broader increment widths (Schöne et al., 2004a, b, 2005a). Since specimens of a given population react similarly to changes in temperature, their average shell growth patterns can be used to estimate climate and hydrological change. Consequently, increment series of specimens with overlapping lifespans can be cross-dated and combined to form longer chronologies covering several centuries (Schöne et al., 2004a, b, 2005a).

2 Material and methods

Similar to other marine (Epstein et al. 1953; Mook & Vogel 1968; Killingley & Berger 1979) and freshwater bivalves (Dettman et al., 1999; Kaandorp et al. 2003; Versteegh et al. 2009; Pfister et al. 2019), *M. margaritifera* forms its shell near equilibrium with the oxygen isotope composition of the water ($\delta^{18}O_w$) (Pfister et al. 2018; Schöne et al. 2005a). If the fractionation of oxygen isotopes between the water and shell carbonate is only temperature-dependent and the temperature during shell formation is known or can be otherwise estimated (e.g., from shell growth rate), reconstruction can be made of the oxygen isotope signature of the water from that of the shell ($\delta^{18}O_s$). We collected ten specimens of the freshwater pearl mussel, *M. margaritifera* from three rivers in Norrland (Norrbottens län), northern Sweden, were used (Fig. 1+2; Table 1). Bivalves were collected between 1993 and 1999 and included nine living specimens and one found dead and articulated (bi-valved; ED-GJ-D6R). Four individuals were taken from the river Nuortejaurbäcken (NJB), two from Grundträsktjärnbäcken (GTB) and four from Görjeån (GJ) (Fig. 1). Since *M. margaritifera* is an endangered species (Moorkens et al., 2018), we refrained from collecting additional specimens that could have covered the time interval since collection and manuscript preparation, but relied on material that we obtained – with permission – for a postdoctoral project of one co-author (AEM, formerly known as Elena Dunca) and the doctoral thesis of another co-author (SMB).

The bedrock in the studied catchments is dominated by orthogneiss and granodiorite. The vegetation at GTB (ca. 90 m a.s.l. [above sea-level]) and GJ (ca. 200 m a.s.l.) consisted of a mixed birch forest, while conifers, shrubs and bushes dominated at NJB (ca. 400 m a.s.l.). The studied rivers were thus rich in humin acids. The studied streams were fed by small upstream open (low-through) lakes.

https://doi.org/10.5194/hess-2019-337
Preprint. Discussion started: 29 July 2019

Hydrology and Earth System Sciences
Discussions

95 **2.1 Sample preparation**

The soft parts were removed immediately after collection and shells were then dried from air. One valve of each specimen was wrapped in a protective layer of WIKO metal epoxy resin #5 and mounted to a Plexiglas cube using Gluetec Multipower plastic welder #3. Shells were then cut perpendicular to the growth lines using a low-speed saw (Buehler Isomet) equipped with a diamond-coated (low-diamond concentration) wafering thin blade (400 µm thickness]. One specimen (ED-NJB-A3R) was cut
100 along the longest axis, all others along the height axis from the umbo to the ventral margin (Fig. 2a). From each specimen, two ca. 3 mm-thick shell slabs were obtained and mounted onto glass slides with the mirroring sides. The latter facilitated the temporal alignment of isotope data measured in one slab to growth patterns determined in the other slab. The shell slabs were ground on glass plates using suspensions of 800 and 1200 grit SiC powder and subsequently polished with Al_2O_3 powder (grain size: 1 µm) on a Buehler G-cloth. Between each grinding step and after polishing, the shell slabs were ultrasonically
105 cleaned with water.

2.2 Shell growth pattern analysis

For growth pattern analysis, one polished shell slab was immersed in Mutvei's solution for 20 min at 37-40° C under constant stirring (Schöne et al., 2005b). After careful rinsing in demineralized water, the stained sections were air-dried under a fume hood. Dyed thick-sections were then viewed under a binocular microscope (Olympus SZX16) equipped with sectoral dark
110 field illumination (Schott VisiLED MC1000) and photographed with a Canon EOS 600D camera (Fig. 2b). The widths of the annual increments were determined to the nearest ca. 1 µm with the image processing software (Panopea, © Peinl and Schöne). Measurements were completed in the outer portion of the outer shell layer (oOSL, prismatic ultrastructure) from the boundary between the oOSL and the inner portion of the outer shell layer (iOSL, nacreous ultrastructure) perpendicularly to the previous annual growth line (Fig. 2c). Annual increment width chronologies were detrended with stiff cubic spline functions and
115 standardized to produce dimensionless measures of growth (standardized growth indices, SGI values) following standard sclerochronological methods (Helama et al., 2006; Butler et al., 3013; Schöne, 2013). Due to low heteroscedasticity, no variance correction was needed (Frank et al., 2007).

2.3 Stable isotope analysis

The other polished shell slab of each specimen was used for stable isotope analysis. To avoid contamination of the shell
120 aragonite powders (Schöne et al., 2016), the cured epoxy resin and the periostracum were completely removed prior to sampling. A total of 1,551 powder samples (32-128 µg) were obtained from the oOSL by means of micromilling under a stereomicroscope at 160 x magnification. An equidistant sampling strategy was applied, i.e., within each annual increment the milling step size was held constant (Schöne et al., 2005c). We used a cylindrical, diamond-coated drill bit (1 mm diameter; Komet/Gebr. Brasseler GmbH and Co. KG, model no. 835 104 010) mounted on a Rexim Minimo drill. While the drilling
125 device was affixed to the microscope, the sample was handheld during sampling. In early ontogenetic years, up to 16 samples

https://doi.org/10.5194/hess-2019-337
Preprint. Discussion started: 29 July 2019

were obtained between successive annual growth lines. In the latest ontogenetic portions of specimens ED-NJB-A2R (last year of life) and ED-GJ-D6R (last nine years of life), each isotope sample represented two to three years.

Stable carbon and oxygen isotopes were measured at the Institute of Geosciences at the University of Frankfurt/Main (Germany). Carbonate powder samples were digested in He-flushed borosilicate exetainers at 72 °C using a water-free phosphoric acid. The released CO_2 gas was then measured in continuous flow mode with a ThermoFisher MAT 253 gas source isotope ratio mass spectrometer coupled to a GasBench II. Stable isotope ratios were corrected against an NBS-19 calibrated Carrara marble ($\delta^{13}C = +2.02$ ‰; $\delta^{18}O = -1.76$ ‰). Results are expressed as parts per thousand (‰) relative to the Vienna Pee Dee Belemnite (V-PDB). The long-term accuracy based on blindly measured reference materials with known isotopic composition is better than 0.05 ‰ for both isotope systems. Note that no correction was applied for differences in fractionation factors of the reference material (calcite) and shells (aragonite), because the paleothermometry equation used below (Eq. 2) did not consider these differences as well (Füllenbach et al., 2015). However, the correction of ca. -0.38 ‰ would be required if $\delta^{18}O$ values of shells and other carbonates were compared with each other.

2.4 Instrumental data sets

Shell growth and isotope data were compared to a set of environmental variables including the station-based winter (DJFM) NAO index (obtained from https://climatedataguide.ucar.edu, last access: 9 April 2019) as well as oxygen isotope values of river water ($\delta^{18}O_w$) and weighted (corrected for precipitation amounts) oxygen isotope values of precipitation ($\delta^{18}O_p$). Data on monthly river water and precipitation came from the Global Network of Isotopes in Precipitation (GNIP) and Rivers (GNIR), available at the International Atomic Energy Agency from their website at https://nucleus.iaea.org/wiser/index.aspx (last access: 1 April 2019). Furthermore, monthly air temperature (T_a) data came from the station Stensele, available at the Swedish Meteorological and Hydrological Institute (https://www.smhi.se). From these data, monthly river water temperature (T_w) was computed by using the summer air-river water temperature conversion by Schöne et al. (2004a), Eq. (1):

$$T_w = 0.8844 \times T_a - 0.8606. \quad (1)$$

2.5 Weighted annual shell isotope data

Since shell growth rate varied during the growing season with fastest biomineralization rates occurring during June and July (Dunca et al., 2005), annual growth increments are biased toward summer, and powder samples taken from the shells at equidistant intervals represent different amounts of time. To compute growing season averages (henceforth referred to as 'annual averages') from such intra-annual shell isotope data ($\delta^{18}O_s$, $\delta^{13}C_s$), weighted (henceforth denoted with an asterisk) annual means are thus needed, i.e., $\delta^{18}O_s$* and $\delta^{13}C_s$* (Schöne et al., 2004a). The relative proportion of time of the growing season represented by each isotope sample was computed from a previously published intra-annual growth curve of juvenile *M. margaritifera* from Sweden (Dunca et al., 2005). For example, if four isotope samples were taken between two winter lines

https://doi.org/10.5194/hess-2019-337
Preprint. Discussion started: 29 July 2019

Hydrology and Earth System Sciences
Discussions

at equidistant intervals, the first sample would represent 22.38 % of the time of the main growing season duration, the second, third and forth 20.28, 24.47 and 32.87 %, respectively (Table 2). Accordingly, the weighted annual mean isotope values ($\delta^{18}O_s$*, $\delta^{13}C_s$*) were calculated by multiplying these numbers (= weights) with the respective $\delta^{18}O_s$ and $\delta^{13}C_s$ values and dividing the sum of the products by 100. The four isotope samples of the example above comprise the time intervals of 23 May–22 June, 23 June–21July, 22 July–25 August, and 26 August–12 October, respectively. Missing isotope data due to lost powder, machine error, air in the exetainer etc. were filled in by linear interpolation in 20 instances. We assumed that the timing and rate of seasonal growth remained nearly unchanged throughout lifetime of the specimens and in the study region (see also Sect. 4).

2.6 Reconstruction of oxygen isotope signatures of river water on annual and intra-annual time-scales

To assess how well the shells recorded $\delta^{18}O_w$ on inter-annual time-scales, the stable oxygen isotope signature of river water ($\delta^{18}O_{wr}$*) during the main growing season ('annual' $\delta^{18}O_{wr}$*) was reconstructed from $\delta^{18}O_s$* data and the arithmetic average of (monthly) river water temperatures, T_w, during the same time interval, i.e., 23 May–12 Oct. Through this approach, the temperature-dependent oxygen isotope fractionation was removed from the $\delta^{18}O_s$* data. For this purpose, the paleothermometry equation of Grossman and Ku (1986; corrected for the VPDB-VSMOW scale difference following Gonfiantini et al., 1995) was solved for $\delta^{18}O_{wr}$*, Eq. (2):

$$\delta^{18}O_{wr}* = \frac{19.43 - 4.34 \times \delta^{18}O_s^* - T_w}{-4.34}. \quad (2)$$

Since air temperature data were only available from 1860 onward, T_w prior to that time were inferred from age-detrended and standardized annual growth increment data (SGI) using a linear regression model similar to that introduced by Schöne et al. (2004a). In the revised model, SGI data of 25 shells from northern Sweden (fifteen published chronologies, provided in the two articles cited above, and ten new chronologies from the specimens studied in the present paper) were regressed against weighted annual water temperature, henceforth referred to as annual T_w*. The annual T_w* data consider variations in seasonal shell growth rate. 6.29, 25.49, 24.52, 21.92, 16.88 and 4.90 % of the annual growth increment were formed in each month from May to October, respectively. The values were multiplied with T_w of the corresponding month and the sum of the products divided by 100 to obtain annual T_w* data. The revised shell growth vs. temperature model is as follows, Eq. (3):

$$T_w^* = 1.45 \times SGI + 8.42. \quad (3)$$

https://doi.org/10.5194/hess-2019-337
Preprint. Discussion started: 29 July 2019

For coherency purposes, we also applied this model to post-1859 SGI values and computed river water temperatures that were subsequently used to estimate $\delta^{18}O_{wr(SGI)}$*.

To assess how well the shells recorded $\delta^{18}O_w$ at intra-annual time-scales, we focused on two shells from NJB (ED-NJB-A4R and ED-NJB-A6R), which provided the highest isotope resolution of ca. one to two weeks per sample during the few years of overlap with GNIP and GNIR data. Note, only for this bivalve sampling locality, monthly instrumental oxygen isotope data were available from the GNIP and GNIR data sets (data by Burgman et al., 1981). The $\delta^{18}O_w$ data were measured in the river Skellefteälven near Slagnäs, ca. 40 km SW of NJB (65°34'59.50"N, 18°10'39.12"E) and covered the time interval of 1973-1980. The $\delta^{18}O_p$ data came from Racksund (66°02'60.00"N, 17°37'60.00"E; ca. 75 km NW of NJB) and covered the time interval of 1975–1979. Since precipitation amounts were not available from Racksund, we computed average monthly precipitation amounts from data recorded at Arjeplog (66°02'60.00"N, 17°53'60.00"E) during 1961–1967. Arjeplog is located ca. 65 km NW of NJB and ca. 12 km W of Racksund. Equation (2) was used to calculate $\delta^{18}O_{wr}$* from individual $\delta^{18}O_s$* and water temperature that existed during the time when the respective shell portion was formed. Intra-annual water temperatures were computed as weighted averages, T_w*, from monthly T_w considering seasonal changes of the shell growth rate. For example, if four powder samples were taken from the shell at equidistant intervals within one annual increment, 6.29 % of the first sample were formed in May and 18.63 % in June (sum ca. 25 %). The average temperature during that time interval is computed with these numbers as follows: (T_w of May × 0.0629 + T_w of June × 0.1863) / 25. 6.86 % of the second sample from that annual increment formed in June and 17.97 % in July. Accordingly, the average temperature was: (T_w of June × 0.0686 + T_w of July × 17.47) / 25 etc. Note that annual $\delta^{18}O_{wr}$* can also be computed from intra-annual $\delta^{18}O_{wr}$*, but this approach is much more time-consuming and complex than the method described further above. Yet, both methods produce nearly identical results.

2.7 Stable carbon isotopes of the shells

Besides the winter and summer NAO index, weighted annual stable carbon isotope data of the shells, $\delta^{13}C_s$*, were compared to shell growth data (SGI chronologies). Since the $\delta^{13}C_s$* could potentially be influenced by ontogenetic effects, the chronologies were detrended and standardized ($\delta^{13}C_{s(d)}$*) following methods typically used to remove ontogenetic age trends from annual increment width chronologies (see e.g., Schöne, 2016). Detrending was accomplished with cubic spline functions capable of removing any directed trend toward higher or lower values through lifetime.

3 Results

The lengths of the annual increment chronologies of *M. margaritifera* from the three studied rivers (Nuortejaurbäcken, Grundträsktjärnbäcken and Görjeån) ranged from 21 to 181 years and covered the time interval of 1819 to 1999 AD (Table 1). Since the umbonal shell portions were deeply corroded and the outer shell layer was missing – a typical feature of long-lived

https://doi.org/10.5194/hess-2019-337
Preprint. Discussion started: 29 July 2019

freshwater bivalves (Schöne et al., 2004a; Fig 2a) – the actual ontogenetic ages of the specimens could not be determined and may have been up to 10 years higher than listed in Table 1.

3.1 Shell growth and temperature

The ten new SGI series from NJB, GTB and GJ were combined with fifteen published annual increment series of *M. margaritifera* from the rivers Pärlälven, Pärlskalsbäcken and Bölsmanån (Schöne et al., 2004a, b, 2005) to a revised Norrland master chronology. During the 50-year calibration interval of 1926–1975 (the same time interval was used in the previous study by Schöne et al., 2004 a, b, 2005), the chronology was significantly ($p < 0.05$) and positively correlated ($R = 0.74$; $R^2 = 0.55$) to the weighted annual river water temperature (T_w*) during the main growing season (Fig. 3). A somewhat stronger correlation was found when the four specimens from GJ were omitted ($R^2 = 0.63$). These values were similar to the previously published coefficient of determination for a stacked record using *M. margaritifera* specimens from rivers across whole Sweden ($R^2 = 0.60$; note that this number is for SGI vs. an arithmetic annual T_w; a regression of SGI against weighted annual T_w returns an R^2 of 0.64).

3.2 Shell stable oxygen isotope data

The shell oxygen isotope curves showed distinct seasonal and inter-annual variations (Fig. 4+5). The former were particularly well developed in specimens from GTB and NJB (Fig. 4), which were sampled with a very high spatial resolution of ca. 30 µm (ED-GTB-A1R, ED-GTB-A2R, ED-NJB-A4R, ED-NJB-A6R). In these shells, up to 16 samples were obtained from single annual increments translating into a temporal resolution of ca. one to two weeks per sample. Typically, the highest $\delta^{18}O_s$ values of each cycle occurred at the winter lines and lowest values about half way between consecutive winter lines (Fig. 4). Largest seasonal $\delta^{18}O_s$ amplitudes of ca. 2.20 ‰ were measured in specimens from GTB (-8.68 to -10.91 ‰) and ca. 1.70 ‰ in shells from NJB (-8.63 to -10.31 ‰).

Weighted annual shell oxygen isotope ($\delta^{18}O_s$*) values fluctuated on decadal time-scales (major common period: ca. 8 years) with amplitudes larger than those occurring on seasonal scales, i.e., ca. 2.50 and 3.00 ‰ in shells from NJB (-8.63 to -11.10 ‰) and GBT (-7.84 to -10.85 ‰), respectively (Fig. 5a+b). The long chronologies from GJ also revealed a century-scale variation with minima in the 1820s and 1960s and maxima in the 1880s and 1990s (Fig. 5c). $\delta^{18}O_s$* curves of specimens from the same locality showed notable agreement in terms of absolute values and visual agreement (running similarity), specifically specimens from NJB and GTB (Fig. 5a+b). However, the longest chronology from GJ showed only little agreement with the remaining three series from that site (Fig 5c). The similarity among the series also changed through time (Fig 5a-c). In some years, the difference between the series was less than 0.20 ‰ at NJB ($N = 4$) and GTB ($N = 2$) (1983) and 0.10 ‰ at GJ (1953; $N = 4$), whereas in other years, differences varied by up to 0.82 ‰ at NJB and 1.00 ‰ at GTB and GJ, respectively. Average shell oxygen isotope chronologies of the three studied rivers exhibited a strong running similarity (passed the

https://doi.org/10.5194/hess-2019-337
Preprint. Discussion started: 29 July 2019

Hydrology and Earth System Sciences
Discussions

250 'Gleichläufigkeitstest' by Baillie and Pilcher, 1983, for $p < 0.001$) and were significantly positively correlated to each other (R^2 values of NJB vs GTB = 0.34, NJB vs GJ = 0.40 and GTB vs GJ = 0.36; all at $p < 0.0001$).

3.3 Shell stable oxygen isotope data and instrumental records

At NJB – the only bivalve sampling site for which measured stream water isotope data were available from nearby localities – May–Oct ranges of reconstructed and instrumental stream water $\delta^{18}O$ between 1973 and 1980 (without 1977 because missing
255 $\delta^{18}O_w$) were in close agreement (shells: 1.95 ‰ vs. stream water: 1.85 ‰; Fig. 6a). During the same time interval, arithmetic means of the shells were -12.48 ± 0.29 ‰ (ED-NJB-A6R) and -12.42 ± 0.34 ‰ (ED-NJB-A4R), whereas the stream water measured -12.33 ± 0.39 ‰. Corresponding median values equaled -12.37 ± 0.36 ‰ (ED-NJB-A6R), -12.30 ± 0.32 ‰ (ED-NJB-A4R), and -12.39 ± 0.30 ‰ (stream water). Also, the inter-annual trends of $\delta^{18}O_{wr}$* and $\delta^{18}O_w$ were similar (Fig. 6a): Values declined by ca. 1.00 ‰ between 1973 and 1977 followed by a slight increase of ca. 0.50 ‰ until 1980. In contrast to
260 the damped stream water signal (average seasonal range during four years for both which stream water and precipitation data were available [1975, 1976, 1978, 1979]: -1.50 ± 0.57 ‰), oxygen isotopes in precipitation exhibited much stronger fluctuations on seasonal (on average, -9.37 ± 2.81 ‰; extreme values of ca. -4.00 and -18.00 ‰; Fig. 6b) and inter-annual time-scales. The means (medians) of $\delta^{18}O_w$ and $\delta^{18}O_p$ were -12.59 ± 0.33 ‰ (-12.60 ± 0.37 ‰) and -12.53 ± 1.05 ‰ (-12.70 ± 1.43 ‰), respectively.

265

Despite the limited number of instrumental data, seasonally averaged $\delta^{18}O_{wr}$* data agreed reasonably well with $\delta^{18}O_w$ and weighted $\delta^{18}O_p$ data (corrected for precipitation amounts), respectively, both in terms of correlation coefficients and absolute values (Table 3); these findings were corroborated by the regression analyses of instrumental $\delta^{18}O_p$ against $\delta^{18}O_w$ (Table 3). For example, the oxygen isotope values of summer (June–Sep) precipitation were significantly ($p < 0.05$) and positively
270 correlated to those of shell carbonate precipitated during the same time interval (95 % explained variability in specimen ED-NJB-A6R, and 97 % in specimen ED-NJB-A4R). Likewise, oxygen isotope values in river water and precipitation during summer were positively correlated to each other, though less significant ($p = 0.097$). Statistically significant relationships were also found for $\delta^{18}O_{wr}$* and and $\delta^{18}O_w$ during the main growing season as well as annual $\delta^{18}O_{wr}$* and Dec-Sep $\delta^{18}O_p$. The underlying assumption for the latter was that the $\delta^{18}O_{wr}$* average reflects the combined $\delta^{18}O_p$ of snow precipitated during the
275 last winter (received as meltwater during spring) and rain precipitated during summer. Instrumental data supported this hypothesis, because stream water $\delta^{18}O$ during the main growing season was highly significantly and positively correlated to Dec-Sep $\delta^{18}O_p$. On the other hand, changes of the isotope signal of winter (Dec–Feb) snow were only weakly and not significantly resembled by changes in river water oxygen isotopes during the snowmelt (May–June) or $\delta^{18}O_{wr}$* in shell portions formed during that time interval (Table 3). During the four years under study (1975, 1976, 1978, 1979), measured and
280 reconstructed stream water $\delta^{18}O$ were nearly identical during the main growing season ($\delta^{18}O_w$ = -12.46 ‰; $\delta^{18}O_{wr}$* = -12.57 ‰ and -12.46 ‰) and during summer ($\delta^{18}O_w$ = -12.39 ‰; $\delta^{18}O_{wr}$* = -12.46 ‰ and -12.20 ‰) (Table 3). In contrast, isotopes in precipitation and river water showed larger discrepancies (see further above and Fig. 6b, Table 3).

https://doi.org/10.5194/hess-2019-337
Preprint. Discussion started: 29 July 2019

Hydrology and Earth System Sciences
Discussions

3.4 Shell stable oxygen isotope data and synoptic circulation patterns (NAO)

Site-specific annual $\delta^{18}O_{wr}$* (and $\delta^{18}O_{wr(SGI)}$*) chronologies (computed as arithmetic averages of all chronologies at a given river) were significantly ($p < 0.05$) positively correlated to NAO indices (Fig. 7; Table 4). In NAO^+ years, the $\delta^{18}O_{wr}$* (and $\delta^{18}O_{wr(SGI)}$*) values were higher than during NAO^- years. The strongest correlation existed between the winter (Dec-Mar) NAO and $\delta^{18}O_{wr}$* (and $\delta^{18}O_{wr(SGI)}$*) at NJB (44 to 49 % explained variability). At GTB, the explained variability ranged between 24 and 27 %, whereas at GJ only 16 to 18 % of the inter-annual $\delta^{18}O_{wr}$* (and $\delta^{18}O_{wr(SGI)}$*) variability was explained by the winter NAO index. Between 1947 and 1991, the time interval for which isotope data were available for all sites, R^2 values were more similar to each other and ranged between 0.27 and 0.46 (Table 4). All sites reflected well-known features of the instrumental NAO index series such as the recent (1970-2000) positive shift toward a more dominant winter NAO, which delivered isotopically more positive winter precipitation to our region of interest (Fig. 7a-c). The correlation between $\delta^{18}O_{wr}$* (and $\delta^{18}O_{wr(SGI)}$*) and the summer (June–Aug) NAO index was much lower than for the winter NAO, but likewise positive and sometimes significant at $p < 0.05$ (Table 4). Between 1947 and 1991, 7 to 16 % of the inter-annual oxygen isotope variability was explained by the summer NAO index.

We have also computed an average $\delta^{18}O_{wr}$* curve for the entire study region (Fig. 8a-c). Since the level (absolute values) of the three rivers differed from other (average $\delta^{18}O_{wr}$* of NJB, GTB and GJ during 1947–1992 were -12.51, -12.21 and -14.16 ‰, respectively), the series were standardized and then arithmetically averaged. The resulting chronology, $\delta^{18}O_{wr(Norrland)}$*, was strongly positively correlated to the winter NAO index (56 % explained variability; Fig. 8a). Despite the limited instrumental dataset, $\delta^{18}O$ of river water and precipitation were likewise strongly positively correlated to the winter NAO index (R^2 values of 0.72 and 0.84, respectively; Fig. 8d+e).

3.5 Shell stable carbon isotope data

Shell stable carbon isotope ($\delta^{13}C_s$) data showed less distinct seasonal variations than $\delta^{18}O_s$, but highest values were often also associated with the winter lines and lowest values occurred between subsequent winter lines (Fig. 4). Largest seasonal amplitudes of ca. 3.90 ‰ were observed in specimens from NJB (-8.21 to -12.10 ‰) and ca. one per mil smaller ranges at GTB (-10.97 to -13.88 ‰).

Weighted annual $\delta^{13}C_s$* curves varied greatly from each other in terms of change through lifetime, among localities and even at the same locality (Fig. 5d-f). Note that all curves started in early youth (below the age of ten), except ED-GJ-A1L and ED-GJ-A3L which began only at a minimum age of 25 and 29, respectively (Table 1). Whereas two specimens from NJB (ED-NJB-A6R, ED-NJB-A4R) showed strong ontogenetic $\delta^{13}C_s$* trends from ca. -8.70 to -12.50 ‰, weaker trends toward more negative values were observed in ED-NJB-A2R (ca. -10.00 to -11.70 ‰) and shells of GTB (ca. -11.50 to -13.00 ‰). Opposite ontogenetic trends occurred in ED-GJ-A1L and ED-GJ-A2R (ca. -15.00 to -12.00 ‰), but no trends at all were found

https://doi.org/10.5194/hess-2019-337
Preprint. Discussion started: 29 July 2019

in ED-NJB-A3R, ED-GJ-A3L and ED-GJ-D6R (fluctuations around -12.00 ‰). All curves were also overlain by some decadal variability (typical periods of 3-6 and 13-16, 60-80 years). Even after detrending and standardization (Fig. 5g-i), no statistically significant correlation at $p < 0.05$ was found between average $\delta^{13}C_{s(d)}$* curves of the three sites (NJB-GTB: $R = -0.11$, $R^2 = 0.01$; NJB-GJ: $R = -0.17$, $R^2 = 0.03$; GTB-GJ: $R = 0.10$, $R^2 = 0.01$). However, at each site, individual curves revealed reasonable visual agreement, specifically at NJB and GTB (Fig. 5g+h). At GJ, the agreement was largely limited to the low frequency oscillations (Fig. 5i).

The detrended and standardized annual shell stable carbon isotope ($\delta^{13}C_{s(d)}$) curves showed little to no statistically significant ($p < 0.05$) agreement with the NAO indices or shell growth rate (SGI values) (Fig. 7; Table 4). A statistically significant, weak negative correlation (10 % explained variability) only existed between $\delta^{13}C_{s(d)}$* and the winter NAO at NJB. Some visual agreement was apparent between $\delta^{13}C_{s(d)}$ and SGI in the low frequency realm. For example, at NJB, faster growth during the mid-1950s, 1970s, 1980s and 1990s fell together with lower $\delta^{13}C_{s(d)}$ values (Fig. 7g). Likewise at GTB, faster shell growth seemed to be inversely linked to $\delta^{13}C_{s(d)}$ values (Fig. 7h).

4 Discussion

4.1 On the benefits of freshwater pearl mussels for stream water $\delta^{18}O$ reconstruction

Our results have shown that shells of freshwater pearl mussels from rivers in northern Scandinavia (fed predominantly by small, open lakes and precipitation) can serve as a long-term, high-resolution archive of the stable oxygen isotope signature of the water in which they lived. With these data are damped relative to precipitation (as a result of the water transit times through the catchment of the stream), the observed and reconstructed stream water isotope signal mirror the seasonal and inter-annual variability in $\delta^{18}O_p$. The NAO and subsequent atmospheric circulation patterns determine the origin of air masses and the $\delta^{18}O$ signal in precipitation.

Compared to lake sediments, which have been used for similar reconstructions at nearby localities (e.g., Hammarlund et al., 2002; Andersson et al., 2010; Rosqvist et al., 2004, 2013), the new archive comes with a number of advantages.

(1) The effect of temperature-dependent oxygen isotope fractionation can be removed from $\delta^{18}O_s$ so that the stable oxygen isotope signature of the water in which the bivalves lived can be computed. This is possible, because the water temperature during shell growth can be reconstructed from shell growth data or instrumental air temperature. Similar studies using lake sediments, however, merely relied on estimates of temperature variability during the formation of diatoms, ostracods etc., and how these temperatures changes affect reconstructions of $\delta^{18}O_w$ (e.g., Rosqvist et al., 2013). Noteworthy, in some of these archives (diatoms), the effect of temperature on the fractionation of oxygen isotopes between the skeleton and the ambient water is still debated (Leng, 2006).

https://doi.org/10.5194/hess-2019-337
Preprint. Discussion started: 29 July 2019

Hydrology and Earth System Sciences
Discussions

(2) *M. margaritifera* precipitates its shell near oxygen isotopic equilibrium with the ambient water, and shell $\delta^{18}O$ reflects stream water $\delta^{18}O$. This may not be the case in all archives, which have previously been used. For example, ostracods possibly exhibit vital effects (Leng and Marshall, 2004).

(3) The shells can provide seasonally to inter-annually resolved data. In the present study, each powder sample typically represented as little as one week up to one full growing season (= one 'year'; mid-May to mid-October; Dunca et al., 2005). In very slow growing shell portions of ontogenetically old specimens, individual samples occasionally covered two or, in exceptional cases, three years of growth which resulted in a reduction of variance. A refined sampling strategy and computer-controlled micromilling could ensure that time-averaging consistently remains below one year.

(4) Each sample taken from the shells can be placed in a precise temporal context. The very season and exact calendar year during which the respective shell portion formed can be determined in shells of specimens with known dates of death based on the seasonal growth curve and annual increment counts. Existing studies suffer from the disadvantage that time cannot be precisely constrained, neither at seasonal nor annual time-scales (unless varved sediments are available). Isotope results can be biased toward a particular season of the year or a specific years within a decade.

(5) The specific sampling method based on micromilling produced uninterrupted isotope chronologies, i.e., no shell portion of the outer shell layer remained un-sampled. Due to the high temporal resolution, bivalve shell-based isotope chronologies can provide insights into inter-annual and decadal-scale paleoclimatic variability. Furthermore, it becomes possible to test hypotheses brought forward in previous studies according to which $\delta^{18}O$ signatures of meteoric water are controlled by the winter and/or summer NAO (e.g., Rosqvist et al., 2007, 2013).

In contrast to bivalve shells, sedimentary archives come with a much coarser temporal resolution. Each sample taken from sediments typically represents the average of several years, and the specific season and calendar year during which the ostracods, diatoms, authigenic carbonates etc. grew remains unknown. On the other hand, the time intervals covered by sedimentary archives are much larger and can reveal century and millennial-scale variations with much less effort than sclerochronology-based records. As such, the two types of archives could complement each other perfectly and increase the understanding past climatic variability.

https://doi.org/10.5194/hess-2019-337
Preprint. Discussion started: 29 July 2019

Hydrology and Earth System Sciences
Discussions

4.2 *M. margaritifera* $\delta^{18}O$ reflects stream water $\delta^{18}O$

Unfortunately, complete records of isotope data of the studied rivers were not available. Such data were required for a direct comparison with those acquired from shells ($\delta^{18}O_{wr}$*) and to determine if the shells were precipitated near oxygen isotopic equilibrium with the ambient water. However, one of the study localities (NJB) is located close to the river Skellefteälven, in which $\delta^{18}O_w$ was irregularly determined between 1973 and 1980 (Fig. 6a) within the framework of the Water Resources Program (WRP). The WRP was jointly lead by the International Atomic Energy Agency and the World Meteorological Organization and aimed to complement the GNIP data set with respective isotope data from rivers worldwide (GNIR). It should be noted that the $\delta^{18}O_w$ data of GNIR merely reflect temporal snapshots, but not actual monthly averages. In fact, the isotope signature of meteoric water can vary significantly on short time-scales (e.g., Darling, 2004; Leng and Marshall 2004; Rodgers et al., 2005). In addition, for some months, no GNIR data were available. In contrast, shell isotope data represent changes in the isotope composition of the water over coherent time intervals ranging from one week to one year (and in few cases two or three years). Due to the specific sampling technique (micromilling), uninterrupted shell oxygen isotope time-series were available. It is thus surprising how well the ranges of intra-annual $\delta^{18}O_{wr}$* data compared to instrumental oxygen isotope data of the river Skellefteälven (Fig. 6a), and that summer averages as well as growing season averages of shells and GNIR were nearly identical (Table 3). Furthermore, in each studied river, individual $\delta^{18}O_{wr}$* series agreed strongly with each other (Fig. 5). All these aspects strongly suggest that shell formation occurred near equilibrium with the oxygen isotope composition of the ambient water, and *M. margaritifera* recorded changes of stream water $\delta^{18}O$. The conclusions are in agreement with previously published results from various different freshwater mussels (e.g., Dettman et al., 1999; Kaandorp et al. 2003; Versteegh et al., 2009) and numerous marine bivalves (e.g., Epstein et al., 1953; Mook and Vogel, 1968; Killingley and Berger, 1979).

4.3 Site-specific and synoptic information recorded in shell oxygen isotopes

Although individual chronologies from a given river compared well to each other with respect to absolute values, the average shell oxygen isotope curves of the three studied sites differed in terms of level (Fig. 5+7). Between 1947 and 1992, the average $\delta^{18}O_{wr}$* values of the three rivers differed by almost 2.00 ‰ (NJB: -12.51 ‰; GTB: -12.21 ‰; GJ: -14.16 ‰). If our interpretation is correct and $\delta^{18}O$ values of the studied margaritiferids reflect the oxygen isotope signature of the water in which they lived, then these numbers reflect hydrological differences in the upstream catchment controlled by a complex set of physiographic characteristics: catchment size and elevation, transit times, upstream lake size and depth controlling the potential for evaporative depletion in ^{16}O, river flux rates, river width and depth, humidity, wind speed, groundwater influx, differences in meltwater influx etc. Detailed monitoring would be required to identify and quantify the actual reason(s) for the observed hydrological differences.

https://doi.org/10.5194/hess-2019-337
Preprint. Discussion started: 29 July 2019

Despite site-specific differences described above, the $\delta^{18}O_{wr}$* chronologies of the three rivers were significantly positively correlated to each other, suggesting that common environmental forcings controlled isotopic changes in the entire study region. Potential candidates that were addressed in previous studies include changes in the isotope composition of precipitation, specifically the amount, origin and air-mass trajectory of winter snow and summer rain, timing of snowmelt as well as condensation temperature (Rosqvist et al., 2013). The latter is probably the most difficult to assess, because no records are available documenting the temperature, height and latitude at which the respective clouds formed. Likewise, we cannot confidently assess the link between the isotope signature of precipitation and stream water because only limited and incoherent datasets are available from the study region. Besides that, data on precipitation amounts were taken from another locality and another time interval. Yet, it is well known that precipitation in northern Scandinavia, particularly during winter, originates from two different sources, the Atlantic and arctic/polar regions (Rosqvist et al., 2013), and the moisture of these air masses is isotopically distinct (Araguás-Araguás et al., 2000; Bowen and Wilkinson, 2002). During NAO^+ years, the sea level pressure difference between the Azores High and the Iceland Low is particularly large resulting in mild, wet winters in central and northern Europe, with strong westerlies carrying heat and moisture across the Atlantic Ocean toward higher latitudes (Hurrell et al., 2003). During NAO^- years, however, westerlies are weaker and the Polar Front is shifted southward, allowing Artic air masses to reach northern Scandinavia. Precipitation originating from the North Atlantic is isotopically heavier ($\delta^{18}O_p$ = -5.00 to -10.00 ‰) than precipitation from subarctic and polar regions ($\delta^{18}O_p$ = -10.00 to -15.00 ‰). Furthermore, changes in air mass properties over northern Europe are controlled by atmospheric pressure patterns in the North Atlantic, particularly the North Atlantic Oscillation during winter (Hurrel, 1995; Hurrell et al., 2003). The positive correlation between $\delta^{18}O_{wr}$* chronologies of the three studied rivers and the winter NAO index (Table 4; Fig. 7a-c, 8a) suggests that the shell isotopes recorded a winter precipitation signal, and this can be explained as follows. A larger proportion of arctic air masses carried to northern Scandinavia during winter resulted in lower $\delta^{18}O_p$, whereas a predominance of North Atlantic air masses caused the opposite. In NAO^+ years, strong westerlies carried North Atlantic air masses far northward so that winter precipitation in northern Sweden had significantly higher $\delta^{18}O_p$ values than during NAO^- years. When the NAO was in its negative state, precipitation originated predominantly from moisture of polar regions which are depleted in ^{18}O, and hence have lower $\delta^{18}O_p$ values. The specific isotope signatures in the rivers was controlled by the snowmelt in spring, where the bivalves recorded the isotope signal of the last winter precipitation in their shells. These hypotheses are supported by the correlation of the few available GNIP and GNIR data with the winter NAO index (Fig. 8d+e). Rosqvist et al. (2007) hypothesized that the summer NAO strongly influences $\delta^{18}O_p$ and thus, the $\delta^{18}O_w$ signature of the open, through-flow lakes in northern Scandinavia. However, our data did not support a profound influence of the summer NAO index on $\delta^{18}O_{wr}$* (Fig. 7d-f), and this conclusion is consistent with other studies likewise suggesting that the summer NAO has a much weaker influence on European climate than the NAO during winter (e.g., Hurrell, 1995).

Following Baldini et al. (2008) and Comas-Bru et al. (2016), northern Sweden is not the ideal place to conduct oxygen isotope-based winter NAO reconstructions. Their model predicted only a weak negative or no correlation between $\delta^{18}O_p$ and

https://doi.org/10.5194/hess-2019-337
Preprint. Discussion started: 29 July 2019

the winter NAO index in our study region (Baldini et al., 2008: Fig. 1; Comas-Bru et al. 2016: Fig. 3a). One possible explanation for this is the limited and temporally incoherent GNIP dataset in northern Sweden. In contrast, $\delta^{18}O$ data of diatoms from open lakes in northern Sweden were strongly linked to the amount of precipitation and $\delta^{18}O_p$, which in turn both change with the predominant state of the NAO (Hammarlund et al., 2002; Andersson et al., 2010; Rosqvist et al., 2004, 2007, 2013). Findings of the present study substantiated these interpretations by providing, for the first time, oxygen isotope time-series with sufficient temporal resolution (annual) and precise temporal control required for a year-to-year comparison with the NAO index.

As Comas-Bru et al. (2016) further suggested, the relationship between $\delta^{18}O_p$ and the winter NAO index is subject to spatial non-stationarities, because the southern pole of the NAO migrates along a NE-SW axis in response to the state of another major atmospheric circulation mode in the North Atlantic realm, known as the East Atlantic Oscillation or East Atlantic Pattern (EA) (Moore and Renfrew, 2012; Moore et al., 2013; Comas-Bru and McDermott, 2014). Like the NAO, the EA is most distinct during winter and describes atmospheric pressure anomalies between the North Atlantic west of Ireland (Low) and the subtropical North Atlantic (High). Through interaction of these circulation patterns, the correlation between the winter NAO and $\delta^{18}O_p$ can weaken at times in certain regions. For example, when both indices are in their positive state, the jet stream shifts poleward (Woolings and Blackburn, 2012) and the storm trajectories that enter Europe in winter take a more northerly route (Comas-Bru et al., 2016). The $\delta^{18}O_p$ values will then be lower than during NAO^+/EA^- years. To identify whether this applies to the study region, we followed Comas-Bru et al. (2016) and tested if the relationship between the winter NAO and reconstructed river water oxygen isotope data remain significant during years when the signs of both indices are the same (EQ) and during years when they are opposite (OP) (note, the EA index is only available from 1950 onward). As demonstrated in Fig. 8b+c, the correlations between the region-wide shell-based oxygen isotope curve ($\delta^{18}O_{wr(Norrland)}$*) and the winter NAO(EQ) ($R = 0.83$, $R^2 = 0.69$, $p < 0.0001$) as well as the winter NAO (OP) ($R = 0.65$, $R^2 = 0.42$, $p = 0.0004$) remain positive and significant above the 95 % confidence level. Hence, in the study region, the relationship between the winter NAO and $\delta^{18}O_{wr}$* is not compromised by the EA; $\delta^{18}O_{wr}$* thus serves as a faithful proxy for the winter NAO index.

4.4 Damped river water oxygen isotope signals

Compared to the large isotopic difference between winter precipitation sourced from SW or N air masses, the huge seasonal spread and inter-annual fluctuations of $\delta^{18}O_p$ (seasonal: ca. -4.00 to -18.00 ‰, Fig. 6b; inter-annual: ca. -10.50 ‰ to -14.40 ‰; Fig. 8e) as well as the predicted seasonal variance of $\delta^{18}O_w$ in the study region (Waterisotopes Database 2019: http://www.waterisotopes.org, last access: 25 May 2019: -8.70 to 17.30 ‰), the observed and shell-derived variance of stream water $\delta^{18}O$ was notably small and barely exceeded 2.00 ‰, both on seasonal (Fig. 6) and inter-annual time-scales (Fig. 5a-c). This figure agrees well with seasonal amplitudes determined in other rivers at higher latitudes of the Northern Hemisphere (Halder et al. 2015) and can broadly be explained by catchment damping effects due to water collection, mixing, storage and release processes in upstream lakes and groundwater from which these rivers were fed. Catchment mean transit time (MTT),

https://doi.org/10.5194/hess-2019-337
Preprint. Discussion started: 29 July 2019

determined via a simple precipitation vs. stream flow isotope signal amplitude damping approach (as per de Walle et al., 1997), is approximately 6 months – corroborating the hypothesis of a mixed snowmelt and precipitation contribution to the stream water $\delta^{18}O$ signal during the growing season.

The attenuated variance on inter-annual time-scales can partly be explained by inter-annual changes in the amount of winter precipitation and the timing of snowmelt. Colder spring temperatures typically resulted in a delayed snowmelt so that lower oxygen isotope signatures still prevailed in the river water when the main growing season of the bivalves started. However, winter precipitation amounts remained below average in NAO^- years, so that the net effect on $\delta^{18}O_w$ in spring was not massive. In contrast, the amount of snow precipitated during NAO^+ years was larger, but milder spring temperatures resulted in an earlier and faster snowmelt, so that the effect on the isotope signature of river water at the beginning of the growing season of the mussels likely remained moderate.

4.5 Sub-annual dating precision and relative changes of seasonal shell growth rate

The precision by which the time can be determined that is represented by individual isotope samples depends on the validity of the seasonal growth model. We assumed that the timing and rate of seasonal shell growth was similar to published data of *M. margaritifera* and remained the same in each year and each specimen. This may not be entirely correct, because the timing and rate of seasonal shell growth can potentially vary between localities, among years and among individuals. A major dating error exceeding four weeks, however, seems unlikely because the oxygen isotope series of individual specimens at each site were in good agreement. Presumably, the timing of seasonal shell growth is controlled by genetically determined biological clocks, which serve to maintain a consistent duration of the growing season. Although shells grew faster in some and slower in other years, the relative seasonal changes of the shell growth likely remained similar and consisted of a gradual increase as the water warmed and more food became available in spring and summer followed by a gradual decline as temperatures dropped in fall. It was further assumed that the timing and rate of shell growth has not significantly changed through the lifetime of the organism. If that was not the case, it would be impossible to crossdate growth curves from young and old individuals and construct master chronologies (Schöne et al., 2004a, b, 2005). Based on these arguments, seasonal dating errors were likely minor.

4.6 Shell stable carbon isotopes

Our results are consistent with previous studies using long-lived bivalves (Beirne et al., 2012; Schöne et al., 2005c, 2011), where $\delta^{13}C_s$ chronologies of *M. margaritifera* did not show consistent ontogenetic trends, but rather oscillated around an average value (ca. -12.00 to -13.00 ‰). The time-series of NJB were too short to reject the hypothesis of directed trends through lifetime, but we propose here that the $\delta^{13}C_s$ of shells from that river would also average out at ca. -12.50 ‰ like at the other two studied sites, if longer chronologies were available. If a contribution of metabolic CO_2 to the shell carbonate exists in this species (which we cannot preclude because no $\delta^{13}C$ values of the dissolved inorganic carbon (DIC) data are available

https://doi.org/10.5194/hess-2019-337
Preprint. Discussion started: 29 July 2019

for the studied rivers), it likely remains constant through lifetime. Observed stable carbon isotope signatures in the mussel shells are in the range of those expected and observed in stream waters of northern Europe (-10.00 to -15.00 ‰; Leng and Marshall, 2004)

Seasonal and inter-annual changes of $\delta^{13}C_s$ could be indicative of changes in primary production, food composition, respiration and influx of terrestrial detritus. However, in the absence of information on how the environment of the studied rivers changed through time, we can only speculate about possible causes of temporal $\delta^{13}C_{DIC}$ variations. For example, increased primary production in the water would not only have propelled shell growth rate, but also resulted in a depletion of ^{12}C in the DIC pool and thus, higher $\delta^{13}C_{DIC}$ and $\delta^{13}C_s$ values. However, just the opposite was observed on seasonal and inter-annual time-scales. Highest $\delta^{13}C_s$ values often occurred near the annual growth lines, i.e., during times of slow growth, and, although not statistically significant, annual $\delta^{13}C_{s(d)}$* at NJB and GTB was inversely related to shell growth rate (Fig. 7g+h; Table 4). Accordingly, $\delta^{13}C_{s(d)}$* does not seem to reflect phytoplankton dynamics. Another possibility is that a change in the composition of mussel food occurred which changed the shell stable carbon isotope values without a statistically significant effect on shell growth rate. Since the isotope signatures of potential food sources differ from each other (e.g., Gladyshev, 2009), a change in relative proportions of phytoplankton, decomposing plant litter from the surrounding catchment vegetation, bacteria, POM deriving from higher organisms etc. could have left a footprint in the $\delta^{13}C_{s(d)}$* values. Furthermore, seasonal and inter-annual changes in respiration or influx of terrestrial detritus may have changed the isotope signature of the DIC pool and thus the shells. Support for the latter comes from the negative correlation between $\delta^{13}C_{s(d)}$* and the winter NAO. After wet (snow-rich) winters (NAO^+ years), stronger terrestrial runoff may have flushed increased amounts of light carbon into the rivers which lowered $\delta^{13}C_{DIC}$ values. To test these hypotheses, data on the stable carbon isotope signature of digested food and DIC would be required, a task for subsequent studies.

5 Summary and conclusions

Stable oxygen isotope values in shells of freshwater pearl mussels, *M. margaritifera*, from rivers in northern Sweden mirror stream water stable oxygen isotope values. Despite a well-known damping of the precipitation signal in stream water isotope records, these mollusks archive local precipitation and synoptic atmospheric circulation signals, specifically the winter NAO. Stable carbon isotope data of the shells are more challenging to interpret, but they seem to record local environmental conditions such as changes in DIC and/or food composition.

The bivalve shell oxygen isotope record presented here extends back to AD 1819, but there is potential for developing longer isotope chronologies through the use of fossil shells of *M. margaritifera* collected in the field or taken from museum collections. With suitable material and by applying the crossdating technique, the existing chronology could probably be extended by several centuries back in time. Stream water isotope records may shed new light on pressing questions related to

https://doi.org/10.5194/hess-2019-337
Preprint. Discussion started: 29 July 2019

climate change impacts on river systems, mechanistic understanding of water flow and quality controlling processes, calibration and validation of flow and transport models, climate and earth system modeling, time variant catchment travel time modeling, etc. Longer and coherent chronologies are essential to reliably identify multidecadal and century-scale climate dynamics. Even individual radiocarbon dated fossil shells that do not overlap with the existing master chronology can provide valuable paleoclimate information, because each specimen of *M. margaritifera* can open a seasonally to annually resolved, multi-year window into the history of rivers.

Acknowledgements. We thank Denis Scholz and Erika Pietroniro for constructive discussions.

Data and code availability. All data and code used in this study are available from the authors on request.

Sample availability. Bivalve shell samples are archived and stored in the paleontological collection of the University of Mainz.

Author contributions. BRS designed the study, performed the analyses and wrote the manuscript; AEM and SMB conducted the field work and collected samples; SMB sampled the shells and temporally aligned the isotope data; JF isotopically analyzed the shell powder; LP conducted MTT calculations. All authors jointly contributed to the discussion and interpretation of the data.

Competing interests. The authors declare that they have no conflict of interest.

Financial support. This study has been made possible through a research grant by the Deutsche Forschungsgemeinschaft DFG to BRS (SCHO793/1).

References

Andersson, S., Rosqvist, G., Leng, M. J., Wastegard, S., and Blaauw, M.: Late Holocene climate change in central Sweden inferred from lacustrine stable isotope data, J. Quat. Sci., 25, 1305–1316, https://doi.org/10.1002/jqs.1415, 2010.

Araguás-Araguás, L., Froehlich, K., and Rozanski, K.: Deuterium and oxygen-18 isotope composition of precipitation and atmospheric moisture, Hydrol. Process., 14, 1341–1355, https://doi.org/10.1002/1099-1085(20000615)14:8<1341::AID-HYP983>3.0.CO;2-Z, 2000.

https://doi.org/10.5194/hess-2019-337
Preprint. Discussion started: 29 July 2019

Baillie, M. G. L., and Pilcher, J. R.: A simple crossdating program for tree-ring research, Tree-ring Bull., 33, 7–14, 1973.

Baldini, L. M., McDermott, F., Foley, A. M., and Baldini, J. U. L.: Spatial variability in the European winter precipitation δ^{18}O-NAO relationship: Implications for reconstructing NAO-mode climate variability in the Holocene, Geophys. Res. Lett., 35, L04709, 6 p., https://doi.org/10.1029/2007GL032027, 2008.

Beirne, E. C., Wanamaker Jr., A. D., and Feindel, S. C.: Experimental validation of environmental controls on the δ^{13}C of *Arctica islandica* (ocean quahog) shell carbonate, Geochim. Cosmochim. Acta 84, 395–409, https://doi.org/10.1016/j.gca.2012.01.021, 2012.

Bowen, G. J., and Wilkinson, B.: Spatial distribution of δ^{18}O in meteoric precipitation, Geology, 30, 315–318, https://doi.org/10.1130/0091-7613(2002)030%3C0315:SDOOIM%3E2.0.CO;2, 2002.

Bowen G. J., Wassenaar L. I., and Hobson K. A.: Global application of stable hydrogen and oxygen isotopes to wildlife forensics, Oecologia, 143, 337–348, doi:10.1007/s00442-004-1813-y, 2005.

Burgman, J. O., Eriksson, E., and Westman, F.: Oxygen-18 variation in river waters in Sweden. Avd. Hydrol. Unpublished Report, Uppsala Univ., Naturgeogr. Inst., 42 p., 1981.

Butler, P. G., Wanamaker Jr., A. D., Scourse, J. D., Richardson, C. A., and Reynolds, D. J.: Variability of marine climate on the North Icelandic Shelf in a 1357-year proxy archive based on growth increments in the bivalve *Arctica islandica*, Palaeogeogr. Palaeoclimatol. Palaeoecol., 373, 141–151, https://doi.org/10.1016/j.palaeo.2012.01.016, 2013.

Comas-Bru, L., and McDermott, F.: Impacts of the EA and SCA patterns on the European twentieth century NAOwinter climate relationship, Quart. J. R. Meteorol. Soc., 140, 354–363, https://doi.org/10.1002/qj.2158, 2014.

Comas-Bru, L., McDermott, F., and Werner, M.: The effect of the East Atlantic pattern on the precipitation δ^{18}O-NAO relationship in Europe, J. Clim. Dyn., 47, 2059–2069, https://doi.org/10.1007/s00382-015-2950-1, 2016.

Darling, W. G.: Hydrological factors in the interpretation of stable isotopic proxy data present and past: a European perspective, Quat. Sci. Rev., 23, 743–770, https://doi.org/10.1016/j.quascirev.2003.06.016, 2004.

Darling, W. G., and Bowes, M. J.: A long-term study of stable isotopes as tracers of processes governing water flow and quality in a lowland river basin, Hydrol. Process., 30, 2178–2195, https://doi.org/10.1016/j.quascirev.2003.06.016, 2016.

https://doi.org/10.5194/hess-2019-337
Preprint. Discussion started: 29 July 2019

Dettman, D. L, Reische, A. K., and Lohmann, K. C.: Controls on the stable isotope composition of seasonal growth bands in aragonitic fresh-water bivalves (unionidae), Geochim. Cosmochim. Acta, 63, 1049–1057, https://doi.org/10.1016/S0016-7037(99)00020-4, 1999.

DeWalle, D. R., Edwards, P. J., Swistock, B. R., Aravena, R., and Drimmie, R. J.: Seasonal isotope hydrology of three Appalachian forest catchments. Hydrol. Process., 11, 1895–1906, https://doi.org/10.1002/(SICI)1099-1085(199712)11:15<1895::AID-HYP538>3.0.CO;2-%23, 1997.

Dunca, E., and Mutvei, H.: Comparison of microgrowth pattern in *Margaritifera margaritifera* shells from south and north Sweden, Am. Malacol. Bull., 16, 239–250, 2001.

Dunca E., Schöne, B.R., and Mutvei, H.: Freshwater bivalves tell of past climates: But how clearly do shells from polluted rivers speak? Palaeogeogr. Palaeoclimatol. Palaeoecol., 228, 43–57, https://doi.org/10.1016/j.palaeo.2005.03.050, 2005.

Epstein S., Buchsbaum R., Lowenstam H. A., and Urey H. C.: Revised carbonate-water isotopic temperature scale, Geol. Soc. Am. Bull., 64, 1315–1326, https://doi.org/10.1130/0016-7606(1953)64[1315:RCITS]2.0.CO;2, 1953.

Frank, D., Esper, J., and Cook, E. R.: Adjustment for proxy number and coherence in a large-scale temperature reconstruction, Geophys. Res. Lett., 34, 5 p., https://doi.org/10.1029/2007GL030571, 2007.

Füllenbach, C. S., Schöne, B. R., and Mertz-Kraus, R.: Strontium/lithium ratio in shells of *Cerastoderma edule* (Bivalvia) - A new potential temperature proxy for brackish environments, Chem. Geol., 417, 341–355, http://dx.doi.org/10.1016/j.chemgeo.2015.10.030, 2015.

Geeza, T. J., Gillikin, D. P., Goodwin, D. H., Evans, S. D., Watters, T., and Warner, N. R.: Controls on magnesium, manganese, strontium, and barium concentrations recorded in freshwater mussel shells from Ohio. Chem. Geol., https://doi.org/10.1016/j.chemgeo.2018.01.001, in press a.

Geeza, T. J., Gillikin, D. P., McDevitt, B., Van Sice, K., and Warner, N. R.: Accumulation of Marcellus Formation oil and gas wastewater metals in freshwater mussel shells. Environ. Sci. Technol., http://dx.doi.org/10.1021/acs.est.8b02727, in press b.

Gladyshev, M. I.: Stable isotope analyses in aquatic ecology (a review), Journal of Siberian Federal University - Biology 4, 381–402, https://doi.org/10.17516/1997-1389-0220, 2009.

https://doi.org/10.5194/hess-2019-337
Preprint. Discussion started: 29 July 2019

640

Gonfiantini, R., Stichler, W., and Rozanski, K.: Standards and intercomparison materials distributed by the International Atomic Energy Agency for stable isotope measurements (IAEA-TECDOC-825), International Atomic Energy Agency (IAEA), Vienna, Austria, 13–29, https://www-pub.iaea.org/MTCD/publications/PDF/te_825_prn.pdf, 1995.

645 Grossman, E. L., and Ku, T.-L.: Oxygen and carbon isotope fractionation in biogenic aragonite; temperature effects, Chem. Geol. Isot. Geosci. Sect., 59, 59–74, https://doi.org/10.1016/0168-9622(86)90057-6, 1986.

Halder, J., Terzer, S., Wassenaar, L. I., Araguás-Araguás, L., and Aggarwal, P. K.: The Global Network of Isotopes in Rivers (GNIR): integration of water isotopes in watershed observation and riverine research, Hydrol. Earth Syst. Sci., 19, 3419–3431,
650 https://doi.org/10.5194/hess-19-3419-2015, 2015.

Hammarlund, D., Barnekow, L., Birks, H. J. B., Buckardt, B., and Edwards, T. W. D.: Holocene changes in atmospheric circulation recorded in the oxygen-isotope stratigraphy of lacustrine carbonates from northern Sweden, Holocene, 12, 339–351, https://doi.org/10.1191%2F0959683602hl548rp, 2002.

655

Helama, S., Schöne, B. R., Black, B.A., and Dunca, E.: Constructing long-term proxy series for aquatic environments with absolute dating control using a sclerochronological approach: introduction and advanced applications, Mar. Freshw. Res., 57, 591–599, https://doi.org/10.1071/MF05176, 2006.

660 Hurrell, J. W.: Decadal trends in the North Atlantic Oscillation: regional temperatures and precipitation, Science, 269, 676–679, https://doi.org/10.1126/science.269.5224.676, 1995.

Hurrell, J. W., Kushnir, Y., Ottersen, G., and Visbeck, M.: An overview of the North Atlantic Oscillation, in: The North Atlantic Oscillation. Climatic Significance and Environmental Impact, edited by: Hurrell, J.W., Kushnir, Y., Ottersen, G., and
665 Visbeck, M., Geophysical Monograph, 134, American Geophysical Union, Washington, DC, U.S.A., 1–35, https://doi.org/10.1029/134GM01, 2003.

Kaandorp, R. J. G., Vonhof, H. B, Del Busto, C., Wesselingh, F. P., Ganssen, G. M., Marmól, A. E., Romero Pittman, L., and van Hinte, J. E.: Seasonal stable isotope variations of the modern Amazonian freshwater bivalve *Anodontites trapesialis*,
670 Palaeogeogr. Palaeoclimatol. Palaeoecol., 194, 339–354, https://doi.org/10.1016/S0031-0182(03)00332-8, 2003.

https://doi.org/10.5194/hess-2019-337
Preprint. Discussion started: 29 July 2019

Kelemen, Z., Gillikin, D. P., Graniero, L. E., Havel, H., Darchambeau, F., Borges, A. V., Yambélé, A., Bassirou, A., and Bouillon, S.: Calibration of hydroclimate proxies in freshwater bivalve shells from Central and West Africa. Geochim. Cosmochim. Acta, 208, 41–62, http://dx.doi.org/10.1016/j.gca.2017.03.025, 2017.

Kelemen, Z., Gillikin, D. P., and Bouillon, S.: Relationship between river water chemistry and shell chemistry of two tropical African freshwater bivalve species. Chem. Geol., https://doi.org/10.1016/j.chemgeo.2018.04.026, in press.

Killingley, J. S., and Berger, W. H.: Stable isotopes in a mollusk shell: detection of upwelling events, Science, 205, 186–188, https://doi.org/10.1126/science.205.4402.186, 1979.

Leng, M. L.: Isotopes in Palaeoenvironmental Research, Developments in Paleoenvironmental Research 10, 1–307, https://doi.org/10.1007/1-4020-2504-1, 2006.

Leng, M. L., and Marshall, J. D.: Palaeoclimate interpretation of stable isotope data from lake sediment archives, Quat. Sci. Rev., 23, 811–831, https://doi.org/10.1016/j.quascirev.2003.06.012, 2004.

Mook, W. G., and Vogel, J. C.: Isotopic equilibrium between shells and their environment, Science, 159, 874–875, https://doi.org/10.1126/science.159.3817.874, 1968.

Moore, G. W. K., and Renfrew, I. A.: Cold European winters: interplay between the NAO and the East Atlantic mode, Atmos. Sci. Lett., 13, 1–8, https://doi.org/10.1002/asl.356, 2012.

Moore, G. W. K., Renfrew, I. A., and Pickart, R. S.: Multidecadal mobility of the North Atlantic Oscillation, J. Clim., 26, 2453–2466, https://doi.org/10.1175/JCLI-D-12-00023.1, 2013.

Moorkens, E., Cordeiro, J., Seddon, M. B., von Proschwitz, T., and Woolnough, D.: *Margaritifera margaritifera* (errata version published in 2018). The IUCN Red List of Threatened Species 2018, e.T12799A128686456, http://dx.doi.org/10.2305/IUCN.UK.2017-3.RLTS.T12799A508865.en, 2018.

Mutvei, H., and Westermark, T.: How environmental information can be obtained from naiad shells, Ecol. Stud., 145, 367–379, https://doi.org/10.1007/978-3-642-56869-5_21, 2001.

Nyström, J., Dunca, E., Mutvei, H., and Lindh, U., Environmental history as reflected by freshwater pearl mussels in the river Vramsån, southern Sweden, Ambio 25, 350–355, https://www.jstor.org/stable/4314490, 1996.

Pfister, L., Thielen, F., Deloule, E., Valle, N., Lentzen, E., Grave, C., Beisel, J.-N., and McDonnell, J. J.: Freshwater pearl mussels as a stream water stable isotope recorder, Ecohydrol., 2018e, e2007, 10 p. https://doi.org/10.1002/eco.2007, 2018.

Pfister, L., Grave, C., Beisel, J.-N., McDonnell, J. J.: A global assessment of freshwater mollusk shell oxygen isotope signatures and their relation to precipitation and stream water. Sci. Rep., 9, 4312, 6 p. https://doi.org/10.1038/s41598-019-40369-0, 2019.

Pulteney, R.: A General View of the Writing of Linnaeus, Payne and White, London, https://doi.org/10.5962/bhl.title.96885, 1781.

Rank, D., Wyhlidal, S., Schott, K., Weigand, S., and Oblin, A.: Temporal and spatial distribution of isotopes in river water in Central Europe: 50 years of experience with the Austrian network of isotopes in rivers, Isotop. Environ. Health Stud., 54, 115–136, https://doi.org/10.1080/10256016.2017.1383906, 2017.

Reckerth, A., Stichler, W., Schmidt, A., and Stumpp, Ch.: Long-term data set analysis of stable isotopic composition in German rivers, J. Hydrol. 552, 718–731, https://doi.org/10.1016/j.jhydrol.2017.07.022, 2017.

Risi, C., Ogée, J., Bony, S., and Kurz Besson, C.: The water isotopic version of the land-surface model ORCHIDEE: Implementation, evaluation, sensitivity to hydrological parameters, Hydrol. Current Res., 7, 258, doi:10.4172/2157-7587.1000258, 2016.

Rodgers, P., Soulsby, C., Waldron, S., and Tetzlaff, D.: Using stable isotope tracers to identify hydrological flow paths, residence times and landscape controls in a mesoscale catchment, Hydrol. Earth Syst. Sci., 9, 139–155, https://doi.org/10.5194/hessd-2-1-2005, 2005.

Rosqvist, G., Jonsson, C., Yam, R., Karlen, W., and Shemesh, A.: Diatom oxygen isotopes in pro-glacial lake sediments from northern Sweden: a 5000 year record of atmospheric circulation, Quat. Sci. Rev., 23, 851–859, https://doi.org/10.1016/j.quascirev.2003.06.009, 2004.

Rosqvist, G. C., Leng, M. J., and Jonsson, C.: North Atlantic region atmospheric circulation dynamics inferred from a late-Holocene lacustrine carbonate isotope record, northern Swedish Lapland, Holocene, 17, 867–873, https://doi.org/10.1177%2F0959683607080508, 2007.

https://doi.org/10.5194/hess-2019-337
Preprint. Discussion started: 29 July 2019

740 Rosqvist, G. C., Leng, M. J., Goslar, T., Sloane, H. J., Bigler, C., Cunningham L., Dadal, A., Bergman, J., Berntsson, A., Jonsson, C., and Wastegård, S.: Shifts in precipitation during the last millennium in northern Scandinavia from lacustrine isotope records, Quat. Sci. Rev., 66, 22–34, https://doi.org/10.1016/j.quascirev.2012.10.030, 2013.

Schöne, B. R.: *Arctica islandica* (Bivalvia): A unique paleoenvironmental archive of the northern North Atlantic Ocean, Global
745 Planet. Change, 111, 199–225, https://doi.org/10.1016/j.gloplacha.2013.09.013, 2013.

Schöne, B. R., and Krause, R. A.: Retrospective environmental biomonitoring – Mussel Watch expanded. Global Planetary Change, 144, http://dx.doi.org/10.1016/j.gloplacha.2016.08.002, 228–251.

750 Schöne, B. R., Dunca, E., Mutvei, H., and Norlund, U. A 217-year record of summer air temperature reconstructed from freshwater pearl mussels (*M. margarifitera*, Sweden), Quat. Sci. Rev., 23, 1803–1816, https://doi.org/10.1016/j.quascirev.2004.02.017, 2004a.

Schöne, B. R., Dunca, E., Mutvei, H., and Norlund, U.: Corrigendum to "A 217-year record of summer air temperature
755 reconstructed from freshwater pearl mussels (*M. margarifitera*, Sweden)" [Quaternary Science Reviews 23 (2004) 1803–1816]. Quat. Sci. Rev., 23, 2057, https://doi.org/10.1016/j.quascirev.2004.07.005, 2004b.

Schöne, B. R., Dunca, E., Mutvei, H., Baier, S., and Fiebig, J.: Scandinavian climate since the late 18th century reconstructed from shells of bivalve mollusks, Z. Dt. Ges. Geowiss., 156, 501–515, https://dx.doi.org/10.1127/1860-1804/2005/0156-0501,
760 2005a.

Schöne, B. R., Dunca, E., Fiebig, J., and Pfeiffer, M.: Mutvei's solution: an ideal agent for resolving microgrowth structures of biogenic carbonates, Palaeogeogr. Palaeoclimatol. Palaeoecol., 228, 149–166, https://doi.org/10.1016/j.palaeo.2005.03.054, 2005b.

765

Schöne, B. R., Fiebig, J., Pfeiffer, M., Gleß, R., Hickson, J., Johnson, A. L. A., Dreyer, W., and Oschmann, W.: Climate records from a bivalved Methuselah (*Arctica islandica*, Mollusca; Iceland), Palaeogeogr. Palaeoclimatol. Palaeoecol., 228, 130–148, https://doi.org/10.1016/j.palaeo.2005.03.049, 2005c.

770 Schöne, B. R., Wanamaker Jr., A. D., Fiebig, J., Thébault, J., and Kreutz, K. J.: Annually resolved $\delta^{13}C_{shell}$ chronologies of long-lived bivalve mollusks (*Arctica islandica*) reveal oceanic carbon dynamics in the temperate North Atlantic during recent centuries, Palaeogeogr. Palaeoclimatol. Palaeoecol., 302, 31–42, https://doi.org/10.1016/j.palaeo.2010.02.002, 2011.

Teranes, J. L., and McKenzie, J. A.: Lacustrine oxygen isotope record of 20th-century climate change in central Europe: evaluation of climatic controls on oxygen isotopes in precipitation, J. Paleolimnol., 26, 131–146, https://doi.org/10.1023/A:1011175701502, 2001.

Trouet, V., Esper, J., Graham, N. E., Baker, A., Scourse, J. D., and Frank, D. C.: Persistent positive North Atlantic Oscillation mode dominated the Medieval Climate Anomaly, Science, 324, 78–80, https://doi.org/10.1126/science.1166349, 2009.

Versteegh, E. A. A., Troelstra, S. R., Vonhof, H. B., and Kroon, D.: Oxygen isotope composition of bivalve seasonal growth increments and ambient water in the rivers Rhine and Meuse, Palaios, 24, 497–504, https://doi.org/10.2110/palo.2008.p08-071r, 2009.

von Hessling, T.: Die Perlmuscheln und ihre Perlen naturwissenschaftlich und geschichtlich; mit Berücksichtigung der Perlengewässer Bayerns, Engelmann, Leipzig, https://doi.org/10.5962/bhl.title.47047, 1859.

Woollings, T., and Blackburn, M.: The North Atlantic jet stream under climate change and its relation to the NAO and EA patterns, J. Clim., 25, 886–902, https://doi.org/10.1175/JCLI-D-11-00087.1, 2012.

Ziuganov, V., San Miguel, E., Neves, R.J., Longa, A., Fernández, C., Amaro, R., Beletsky, V., Popkovitch, E., Kaliuzhin, S., and Johnson, T.: Life span variation of the freshwater pearl shell: A model species for testing longevity mechanisms in animals, Ambio, 29, 102–105, https://doi.org/10.1579/0044-7447-29.2.102, 2000.

https://doi.org/10.5194/hess-2019-337
Preprint. Discussion started: 29 July 2019

Hydrology and Earth System Sciences
Discussions

795

Table 1: Shells of *Margaritifera margaritifera* from three rivers in northern Sweden used in present study for isotope and growth pattern analysis. Last set of digits denotes whether bivalves were collected alive (a) or dead (d), specimen number and which valve was used (R = right, L = left). § = minimum estimate of lifespan. L = last sampled year incomplete. A = Add ten years to these values to obtain approximate ontogenetic years.

800

River name	Specimen ID	Coordinates and elevation	Age[§] (yr)	Life during year AD	# isotope samples (coverage of years[A])
Nuortejaurbäcken	ED-NJB-A6R	65°42'13.22"N, 19°02'31.01"E, ca. 400 m a.s.l.	22	1972-1993	175 (1-22[i])
	ED-NJB-A4R		27	1967-1993	154 (2-27[i])
	ED-NJB-A2R		48	1946-1993	78 (2-48[i])
	ED-NJB-A3R		24	1970-1993	50 (1-24[i])
Grundträsktjärnbäcken	ED-GTB-A1R	66°02'59.98"N, 22°05'02.25"E, ca. 90 m a.s.l.	51	1943-1993	368 (2-49)
	ED-GTB-A2R		51	1943-1993	315 (3-49)
Görjeån	ED-GJ-A1L	66°20'30.77"N, 20°30'15.02"E, ca. 200 m a.s.l.	80	1916-1997	56 (25-80[i])
	ED-GJ-A2R		82	1918-1997	76 (1-78)
	ED-GJ-A3L		123	1875-1997	110 (29-122)
	ED-GJ-D5L		181	1819-1999	169 (1-180)

https://doi.org/10.5194/hess-2019-337
Preprint. Discussion started: 29 July 2019

Hydrology and Earth System Sciences
Discussions

Table 2: Weights for isotope samples of *Margaritifera margaritifera*. Due to variations of seasonal shell growth rate, each isotope sample taken at equidistant intervals represents different amounts of time. To calculate seasonal or annual averages from individual isotope data, the relative proportion of time of the growing season contained in each sample must be considered when weighted averages are computed. The duration of the growing season comprises 143 days and covers the time interval of 23 May to 12 October.

Number of isotope samples per annual increment	Weight of nth isotope sample (%) within an annual increment; direction of growth to the right (increasing numbers)															
	1st	2nd	3rd	4th	5th	6th	7th	8th	9th	10th	11th	12th	13th	14th	15th	16th
1	100.00															
2	42.66	57.34														
3	27.97	31.47	40.56													
4	22.38	20.28	24.47	32.87												
5	18.18	15.39	18.88	20.27	27.28											
6	15.38	12.59	14.69	16.78	18.18	22.38										
7	13.29	11.88	11.19	13.29	13.99	16.08	20.28									
8	11.59	10.79	9.09	11.19	12.58	11.89	14.69	18.18								
9	10.49	9.79	7.69	9.09	10.49	11.89	10.49	13.29	16.78							
10	9.79	8.39	7.69	7.70	9.09	9.78	9.80	10.49	11.89	15.38						
11	9.09	7.69	7.70	5.59	7.69	8.39	9.79	8.40	10.49	10.48	14.69					
12	8.39	6.99	7.00	5.59	6.99	7.70	8.39	8.39	7.69	10.49	9.09	13.29				
13	7.69	6.30	6.99	5.59	5.60	6.29	7.69	8.40	6.99	7.69	9.79	8.39	12.59			
14	7.69	5.60	6.29	5.59	4.90	6.29	6.30	6.99	6.99	7.70	6.28	9.10	8.39	11.89		
15	6.29	6.30	5.59	5.60	4.19	5.60	5.59	6.99	6.30	6.99	6.29	7.00	8.38	7.70	11.19	
16	6.29	5.60	5.59	4.90	4.19	4.90	5.59	5.60	6.29	4.90	7.69	5.59	7.70	6.99	7.69	10.49

https://doi.org/10.5194/hess-2019-337
Preprint. Discussion started: 29 July 2019

Hydrology and Earth System Sciences
Discussions

Table 3: Relationship between stable oxygen isotope values in precipitation, river water and shells of *Margaritifera margaritifera* from Nuortejaurbäcken during different seasons of the year. The rationale behind the comparison of $\delta^{18}O$ values of winter precipitation and spring river water or shell carbonate is that the isotope signature of meltwater may have left a signal in the water.

		$\delta^{18}O_p$ (Racksund)			$\delta^{18}O_w$ (Skellefteälven)		
	Season	Dec_{t-1}-Sep_t -11.90 ‰	June-Sep -11.09 ‰	Dec_{t-1}-Feb_t -14.10 ‰	May-Oct -12.46 ‰	June-Sep -12.39 ‰	May-June -13.08 ‰
$\delta^{18}O_w$ Skellefteälven	May-Oct -12.46 ‰	**R = 0.90 R^2 = 0.85 *p = 0.050* N = 4**					
	June-Sep -12.39 ‰		R = 0.90 R^2 = 0.82 *p = 0.097* N = 4				
	May-June -13.08 ‰			R = 0.89 R^2 = 0.78 *p = 0.115* N = 4			
$\delta^{18}O_{wr}$* ED-NJB-A6R	May-Oct -12.57 ‰	**R = 1.00 R^2 = 1.00 *p = 0.001* N = 4**			**R = 0.99 R^2 = 0.97 *p = 0.014* N = 4**		
	June-Sep -12.46 ‰		**R = 0.98 R^2 = 0.95 *p = 0.023* N = 4**			R = 0.83 R^2 = 0.68 *p = 0.175* N = 5	
	May-June -12.45 ‰			R = 0.29 R^2 = 0.08 *p = 0.711* N = 4			R = 0.44 R^2 = 0.19 *p = 0.561* N = 4
$\delta^{18}O_{wr}$* ED-NJB-A4R	May-Oct -12.46 ‰	**R = 0.98 R^2 = 0.97 *p = 0.017* N = 4**			**R = 0.99 R^2 = 0.98 *p = 0.008* N = 4**		
	June-Sep -12.20 ‰		**R = 0.98 R^2 = 0.97 *p = 0.017* N = 4**			R = 0.92 R^2 = 0.85 *p = 0.080* N = 4	
	May-June -12.37 ‰			R = 0.78 R^2 = 0.67 *p = 0.244* N = 4			R = 0.90 R^2 = 0.80 *p = 0.105* N = 4

https://doi.org/10.5194/hess-2019-337
Preprint. Discussion started: 29 July 2019

Hydrology and Earth System Sciences
Discussions
Open Access
EGU

820 **Table 4: Site-specific annual isotope chronologies of *Margaritifera margaritifera* shells linearly regressed against winter and summer NAO (wNAO, sNAO) as well as detrended and standardized shell growth rate (SGI). $\delta^{18}O_{wr}$* data were computed from shell oxygen isotope data and temperature data computed from instrumental air temperatures, whereas in the case of $\delta^{18}O_{wr(SGI)}$* data, temperatures were estimated from a growth-temperature model. See text for details. Statistically significant values ($p < 0.05$) are bold.**

	$\delta^{18}O_{wr}$*			$\delta^{18}O_{wr(SGI)}$*			$\delta^{13}C_{s(d)}$*		
	NJB	GTB	GJ	NJB	GTB	GJ	NJB	GTB	GJ
wNAO (DJFM)	**R = 0.67** **R^2 = 0.44** *p < 0.0001*	**R = 0.49** **R^2 = 0.24** *p = 0.0003*	**R = 0.39** **R^2 = 0.16** *p < 0.0001*	**R = 0.70** **R^2 = 0.49** *p < 0.0001*	**R = 0.52** **R^2 = 0.27** *p < 0.0001*	**R = 0.42** **R^2 = 0.18** *p < 0.0001*	R = -0.18 R^2 = 0.03 *p = 0.237*	**R = -0.31** **R^2 = 0.10** *p = 0.034*	R = 0.10 R^2 = 0.01 *p = 0.231*
wNAO (DJFM) 1947-1991	**R = 0.65** **R^2 = 0.43** *p < 0.0001*	**R = 0.52** **R^2 = 0.27** *p < 0.0001*	**R = 0.60** **R^2 = 0.36** *p < 0.0001*	**R = 0.68** **R^2 = 0.46** *p < 0.0001*	**R = 0.56** **R^2 = 0.31** *p < 0.0001*	**R = 0.65** **R^2 = 0.42** *p < 0.0001*	R = -0.18 R^2 = 0.03 *p = 0.237*	**R = -0.31** **R^2 = 0.10** *p = 0.034*	R = 0.10 R^2 = 0.01 *p = 0.231*
sNAO (JJA)	**R = 0.38** **R^2 = 0.14** *p = 0.0097*	**R = 0.40** **R^2 = 0.16** *p = 0.0046*	**R = 0.20** **R^2 = 0.04** *p = 0.0237*	**R = 0.29** **R^2 = 0.09** *p = 0.0491*	**R = 0.34** **R^2 = 0.11** *p = 0.0193*	R = 0.02 R^2 = 0.00 *p = 0.8111*	R = 0.12 R^2 = 0.01 *p = 0.431*	R = 0.01 R^2 = 0.00 *p = 0.936*	R = 0.03 R^2 = 0.00 *p = 0.691*
sNAO (JJA) 1947-1991	**R = 0.36** **R^2 = 0.13** *p = 0.0143*	**R = 0.40** **R^2 = 0.16** *p = 0.0069*	**R = 0.38** **R^2 = 0.14** *p = 0.0116*	R = 0.27 R^2 = 0.07 *p = 0.0734*	**R = 0.32** **R^2 = 0.10** *p = 0.0321*	R = 0.26 R^2 = 0.07 *p = 0.0864*	R = 0.12 R^2 = 0.01 *p = 0.431*	R = 0.01 R^2 = 0.00 *p = 0.936*	R = 0.03 R^2 = 0.00 *p = 0.691*
SGI							R = -0.28 R^2 = 0.08 *p = 0.0634*	R = -0.23 R^2 = 0.05 *p = 0.1161*	R = 0.09 R^2 = 0.01 *p = 0.2333*
SGI 1947-1991							R = -0.27 R^2 = 0.07 *p = 0.0699*	R = -0.22 R^2 = 0.05 *p = 0.5038*	R = 0.10 R^2 = 0.01 *p = 0.5144*

825

https://doi.org/10.5194/hess-2019-337
Preprint. Discussion started: 29 July 2019

Hydrology and Earth System Sciences
Discussions
Open Access
EGU

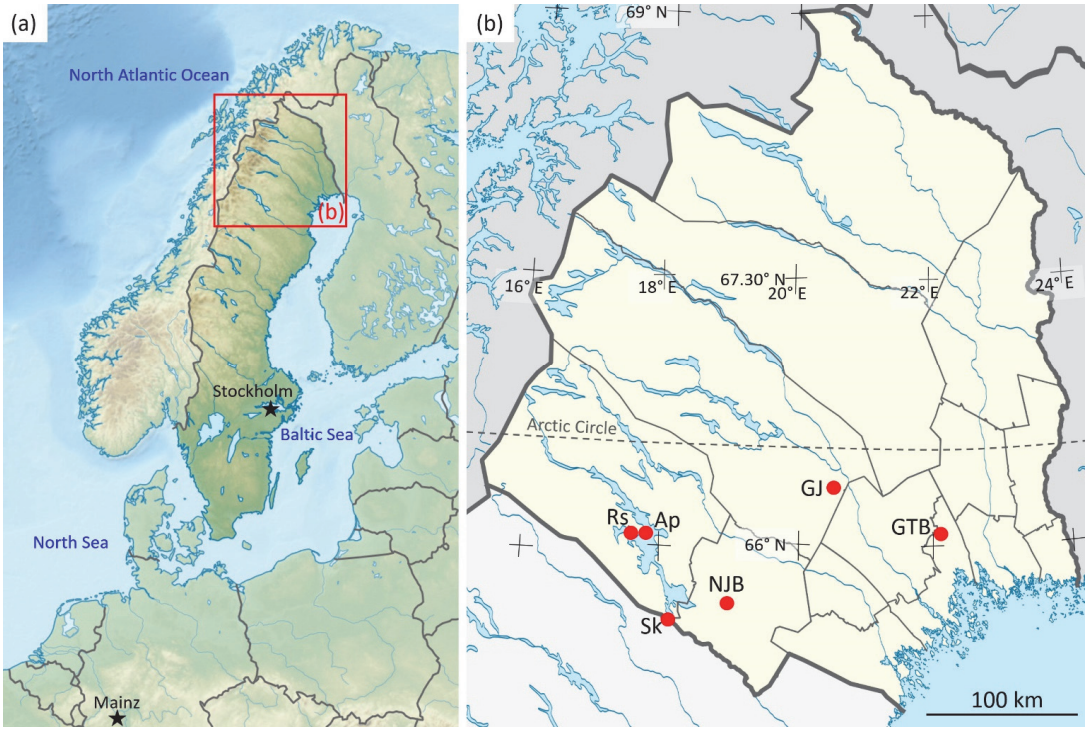

Figure 1: Maps showing sample sites in northern Sweden. (a) Topographic map of Scandinavia. (b) Enlargement of red box in (a) showing Norrbottens län (yellow), a province in northern Sweden, and localities where bivalve shells (*Margaritifera margaritifera*) were collected and isotopes in rivers and precipitation were measured. Shell collection sites: NJB = Nuortejaurbäcken, GTB = Grundträsktjärnbäcken, GJ = Görjeån; GNIR site: Sk = River Skellefteälven near Slagnäs; GNIP sites: Rs = Racksund and Ap = Arjeplog. Basemap of A is by TUBS and used under Creative Commons: https://commons.wikimedia.org/wiki/File:Sweden_in_Europe_(relief).svg. Basemap of B is by Erik Frohne (redrawn by Silverkey) and used under Creative Commons: https://commons.wikimedia.org/wiki/File:Sweden_Norrbotten_location_map.svg.

https://doi.org/10.5194/hess-2019-337
Preprint. Discussion started: 29 July 2019

Hydrology and Earth System Sciences
Discussions
Open Access
EGU

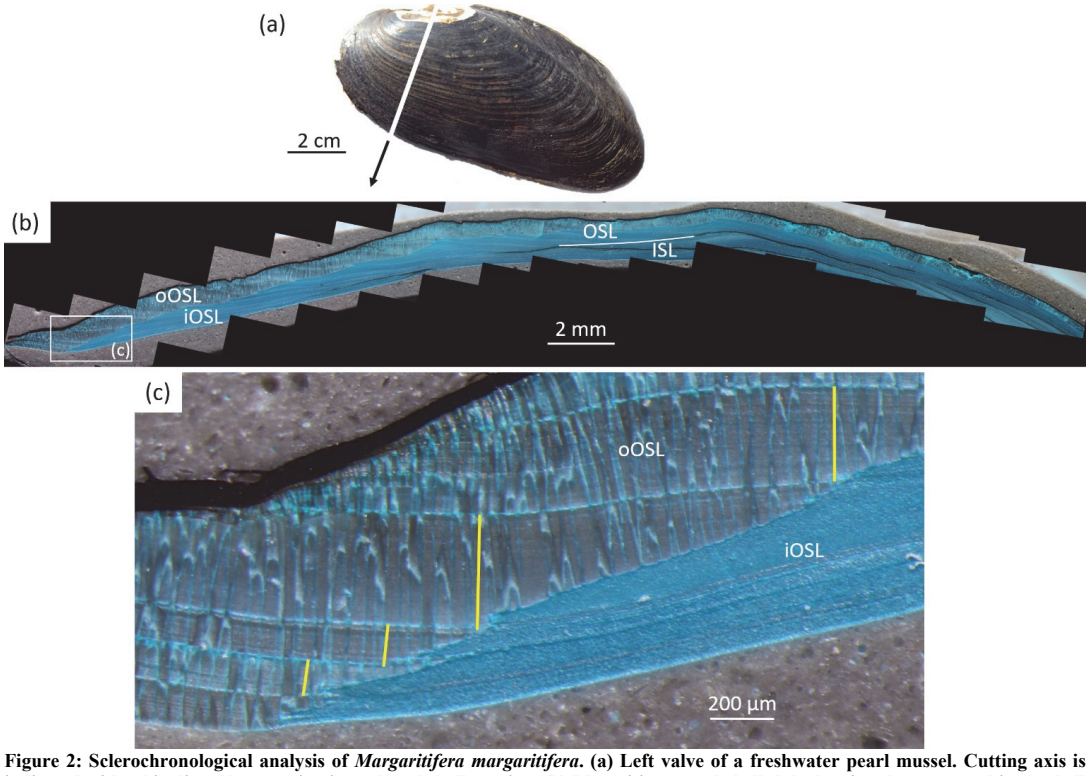

Figure 2: Sclerochronological analysis of *Margaritifera margaritifera*. (a) Left valve of a freshwater pearl mussel. Cutting axis is indicated with white line. Note erosion in umbonal shell portion. (b) Mutvei-immersed shell slab showing the outer and inner shell layers (OSL, ISL) separated by the myostracum (white line). The OSL is further subdivided into an outer and inner portion (oOSL, iOSL). ISL and iOSL consist of nacreous ultrastructure, the oOSL of prismatic ultrastructure. (c) Enlargement of B shows annual growth patterns. Annual increment width measurements (yellow) were completed as perpendiculars from the intersection of the oOSL and iOSL toward the next annual growth line.

https://doi.org/10.5194/hess-2019-337
Preprint. Discussion started: 29 July 2019

Hydrology and Earth System Sciences
Discussions
Open Access
EGU

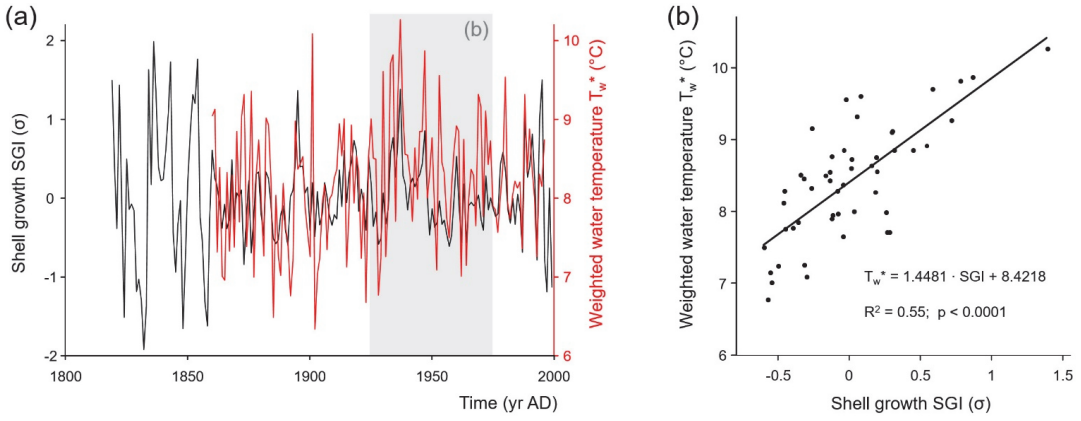

Figure 3: Age-detrended and standardized annual shell growth rate (SGI values) and water temperature during the main growing season (23 May–12 October). (a) Time-series; (b) Cross-plot. Water temperatures were computed from monthly air temperature data using a published transfer function and considering seasonally varying rates of shell growth. Grey box in (a) denotes 50-year calibration interval from which the temperature model (b) was constructed. As seen from the cross-plot in (b), 55 % of the variations in annual shell growth was highly significantly explained by water temperature. Higher temperature resulted in faster shell growth.

https://doi.org/10.5194/hess-2019-337
Preprint. Discussion started: 29 July 2019

Hydrology and Earth System Sciences
Discussions

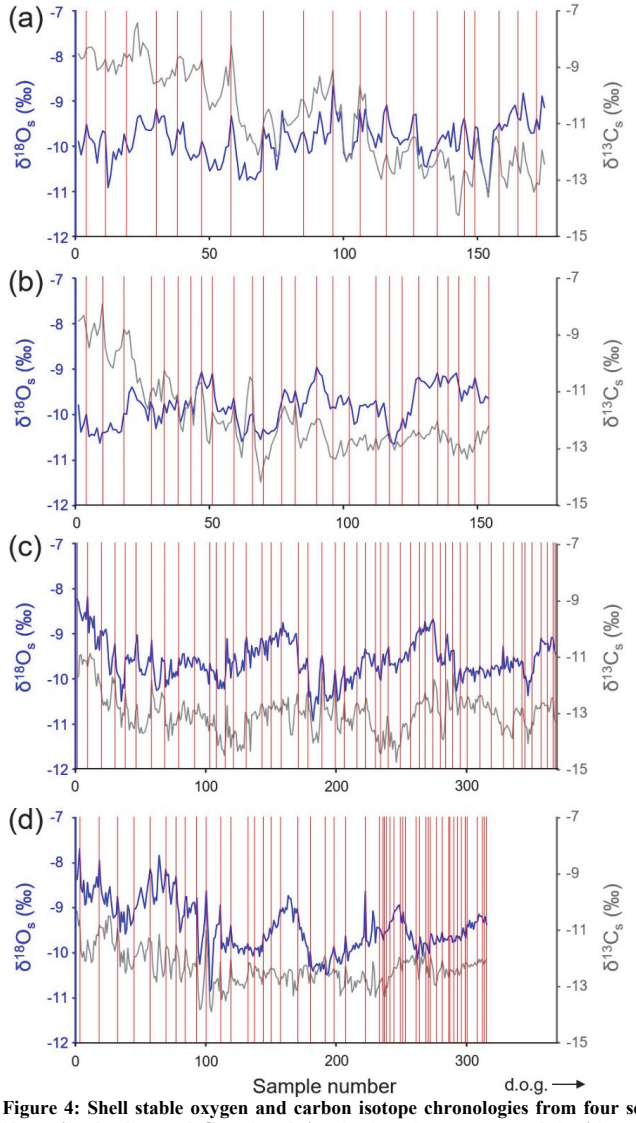

Figure 4: Shell stable oxygen and carbon isotope chronologies from four selected specimens of *Margaritifera margaritifera* from Nuortejaurbäcken and Grundträsktjärnbäcken that were sampled with very high spatial resolution. Individual isotope samples represent time intervals of a little as six days to two weeks in ontogenetically young shell portions and up to one full growing season in the last few years of life. Red vertical lines stand for annual growth lines. (a): ED-NJB-A6R; (b) ED-NJB-A4R; (c) ED-GTB-A1R; (d) ED-GTB-A2R. Since the umbonal shell portions are corroded, the exact ontogenetic age at which the chronologies start cannot be provided. Assuming that the first ten years of life are missing, sampling in (a) started in year eleven, in (b) and (c) in year twelve and in (d) in year thirteen. See also Table 1.

https://doi.org/10.5194/hess-2019-337
Preprint. Discussion started: 29 July 2019

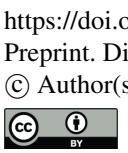

Hydrology and Earth System Sciences
Discussions
Open Access
EGU

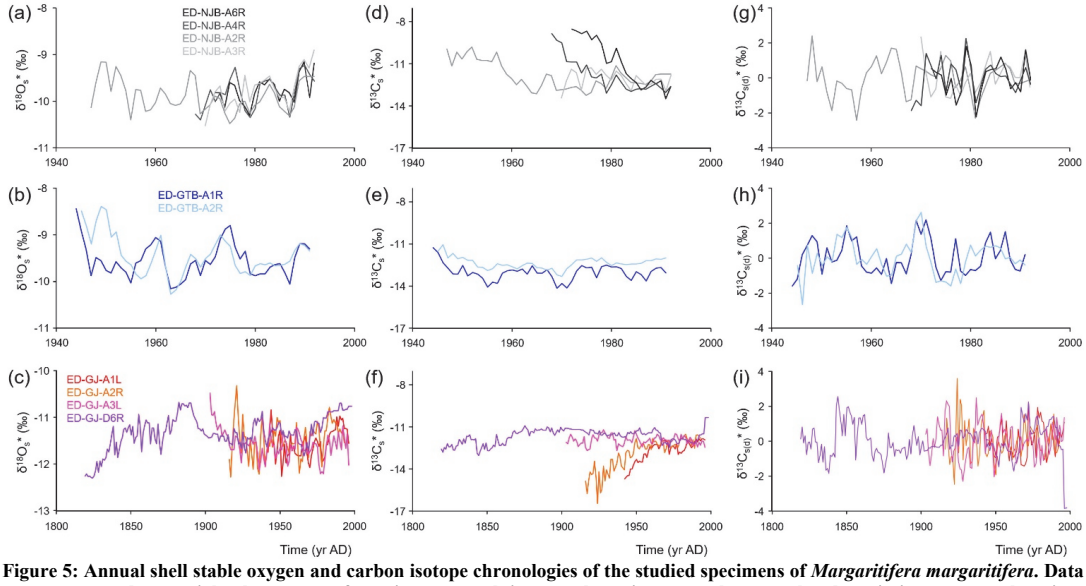

Figure 5: Annual shell stable oxygen and carbon isotope chronologies of the studied specimens of *Margaritifera margaritifera*. Data were computed as weighted averages from intra-annual isotope data, i.e., growth rate-related variations were taken into consideration. First row (a, d, g) = river Nuortejaurbäcken; second row (b, e, h) = Grundträsktjärnbäcken; third row (c, f, i) = Görjeån. (a-c) = oxygen iotopes; (d-f) = carbon isotopes; (g-i) = Detrended and standardized carbon isotopes.

https://doi.org/10.5194/hess-2019-337
Preprint. Discussion started: 29 July 2019

Hydrology and Earth System Sciences
Discussions

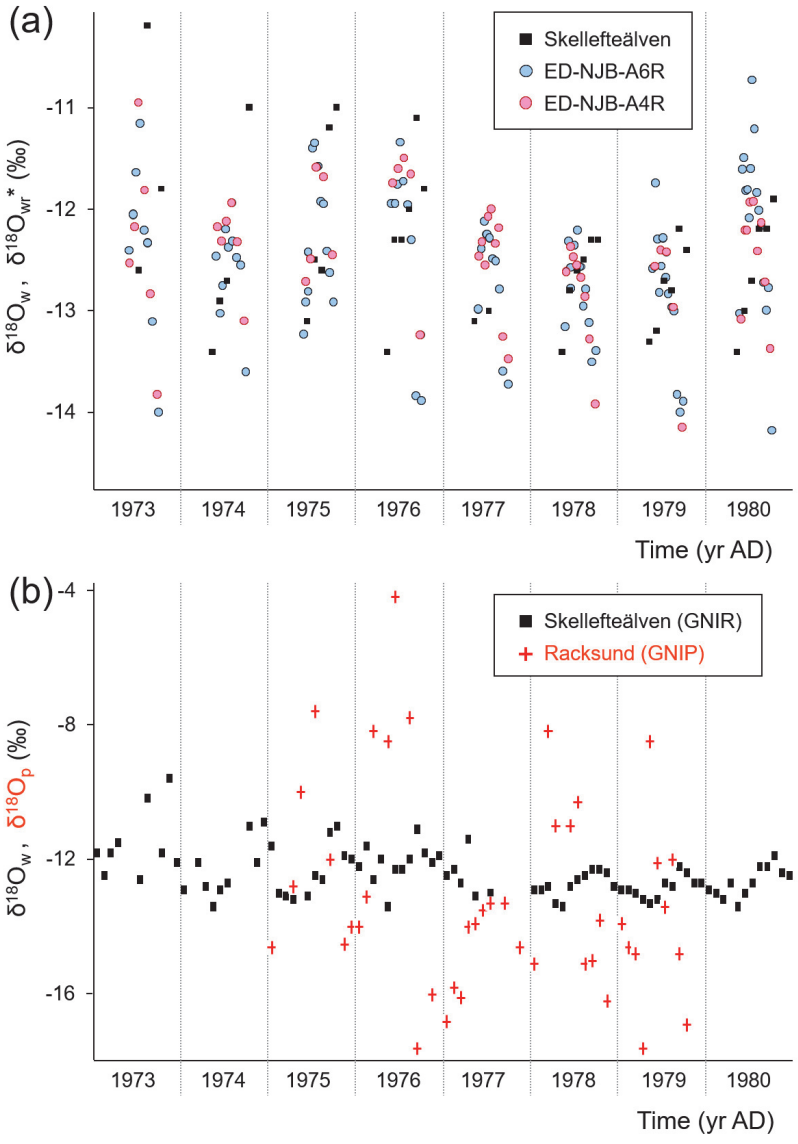

865 **Figure 6: Intra-annual stable oxygen isotope values (1973–1980). (a) Monthly isotopes measured in the river Skellefteälven (May–Oct) and weighted seasonal averages ($\delta^{18}O_{wr}$*) of two shells (*Margaritifera margaritifera*) from Nuortejaurbäcken (see Fig. 1). Note good agreement of level and seasonal ranges of instrumental and reconstructed oxygen isotope data as well as similar inter-annual changes. (b) Comparison of monthly oxygen isotope data in stream water (river Skellefteälven; May–Oct) and precipitation (Racksund; whole year).**

https://doi.org/10.5194/hess-2019-337
Preprint. Discussion started: 29 July 2019

Hydrology and Earth System Sciences
Discussions
Open Access
EGU

870

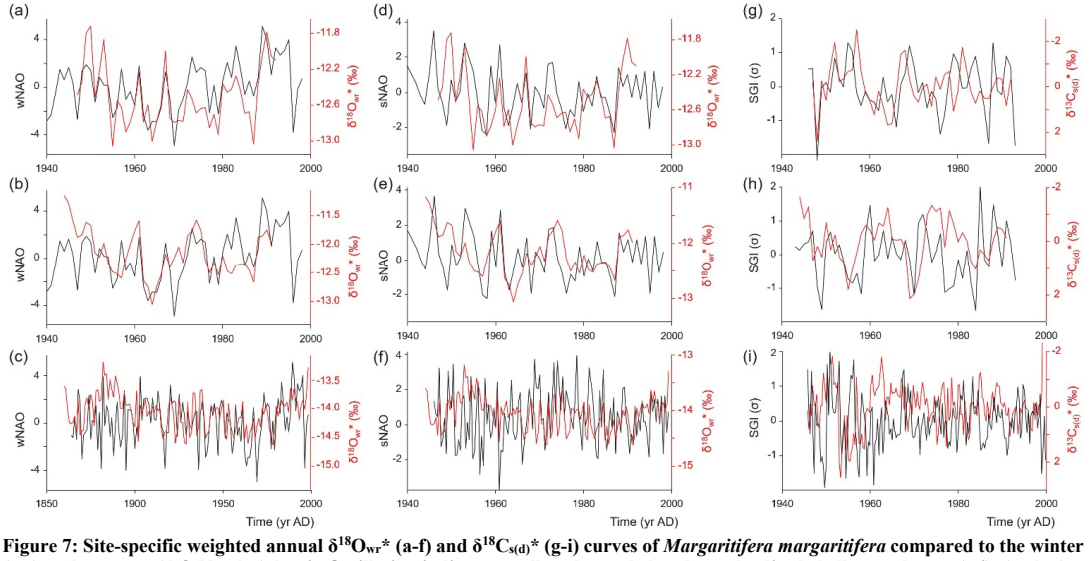

Figure 7: Site-specific weighted annual $\delta^{18}O_{wr}$* (a-f) and $\delta^{18}C_{s(d)}$* (g-i) curves of *Margaritifera margaritifera* compared to the winter (a-c) and summer (d-f) North Atlantic Oscillation indices as well as detrended and standardized shell growth rate (g-i). (a, d, g) = Nuortejaurbäcken; (b, e, h) = Grundträsktjärnbäcken; (c, f, i) = Görjeån.

875

https://doi.org/10.5194/hess-2019-337
Preprint. Discussion started: 29 July 2019

Hydrology and Earth System Sciences
Discussions
Open Access
EGU

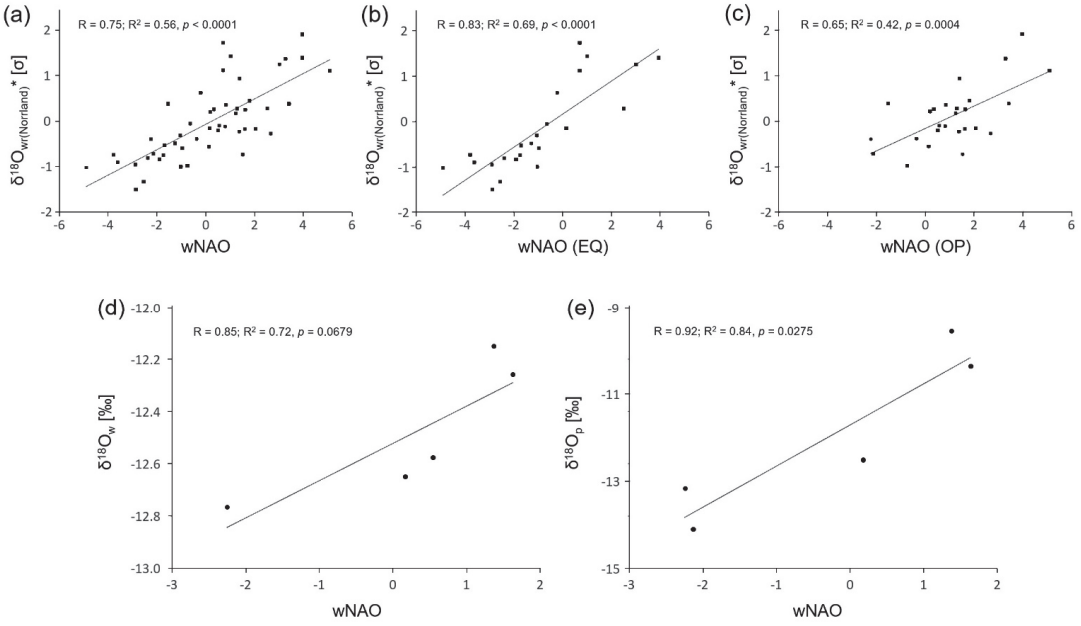

Figure 8: Oxygen isotope data compared to winter NAO index. (a) Standardized $\delta^{18}O_{wr}$* chronology of the study region compared to the winter NAO index between 1950 and 1998. (b) Same as in (a), but only when the East Atlantic Pattern (EA) index has the same sign (EQ) as the winter NAO. (c) Same as in A, but only for cases when the EA index is in the opposite (OP) mode than the winter NAO. (d) $\delta^{18}O_w$ of the river Skelleteälven (during the growing season of the mussels: May–Oct) in comparison to the winter NAO index (1975–1980). (e) $\delta^{18}O$ of precipitation (Dec–Sep) measured at Racksund in comparison to the winter NAO index (1975–1979).